ANALYTICAL AND EXPERIMENTAL INVESTIGATION OF ORTHOGONAL TURN-MILLING PROCESSES

by

EMRE UYSAL

Submitted to the Graduate School of Engineering and Natural Sciences

in partial fulfillment of the requirements for the degree of

Master of Science

Sabanci University

January 2015

ANALYTICAL AND EXPERIMENTAL INVESTIGATION OF ORTHOGONAL TURN-MILLING PROCESSES

APPROVED BY:

Prof. Dr. Erhan Budak
(Dissertation Supervisor)

Assoc. Prof. Bahattin Koç

Assoc. Prof. Mustafa Bakkal

DATE OF APPROVAL: 05.01.2015

To my family

and

my deceased grandfather Şükrü Uysal

ANALYTICAL AND EXPERIMENTAL INVESTIGATION OF ORTHOGONAL TURN-MILLING PROCESSES

Emre Uysal

Industrial Engineering, MS Thesis, 2015

Thesis Supervisor: Prof. Dr. Erhan Budak

Abstract

Machining of hard-to-cut materials is challenging due to their high strength resulting in reduced productivity and high manufacturing cost. Conventional machining processes are commonly used for production of these parts where cutting speed, and thus the material removal rate, is limited due to high tool wear rate. Because of the increasing market demands for higher quality, reduced lead times and cost, alternative techniques are required in order to increase productivity in machining of these materials. An increase in potential production capacity was observed in the recent years due to advancements in machine tools that offer high precision, increased flexibility and spindle speed. Multi-axis machining, which can be a remedy for these demands, have been continuing to spread rapidly in many industries particularly in aerospace and defense. These processes are generally performed on multi-tasking machines through simultaneous cutting operations on the same part or machining of more than one part simultaneously.

Turn-milling, which is a promising multi-axis cutting process combining two conventional machining operations; turning and milling, can offer high productivity for difficult-to-cut materials such as Ti and Ni alloys as well as parts with large diameters which cannot be rotated at high speeds on conventional lathes. However, the work done on analysis and modeling of turn-milling operations is very limited. On the other hand,

due to the high flexibility and capability of turn-milling operations, there are numerous process parameters which need to be selected properly to utilize the full potential offered by these processes. In order to achieve this, process models which consider all cutting parameters are required. In this thesis, analytical models for turn-milling process geometry, chip formation and cutting force including eccentricity effects are presented. Furthermore, circularity, cusp height and surface roughness are modeled and simulated. Model predictions are verified by experiments carried out on a multi-tasking machine tool under different process conditions. Tool wear tests for hard-to-machine materials are also performed on the same machine where effects of turn-milling process conditions on tool life are shown. Simulation and experimental results show that substantial increase in productivity can be achieved using turn-milling in machining of difficult-to-cut materials when process conditions are selected properly.

DİK FREZE İLE TORNALAMA SÜREÇLERİNİN ANALİTİK VE DENEYSEL OLARAK İNCELENMESİ

Emre Uysal

Endüstri Mühendisliği, Yüksek Lisans Tezi, 2015

Tez Danışmanı: Prof. Dr. Erhan Budak

Anahtar Kelimeler: Çok Eksenli Kesme Operasyonu, Dik Freze ile Tornalama, Eksantriklik, Süreç Modelleme, Süreç Benzetimi, Form Hatası, Takım Ömrü

Özet

Kesilmesi zor malzemelerin talaşlı işlenmesi, üretim verimliliklerini düşüren ve üretim maliyetlerini arttıran yüksek sertlikleri nedeniyle bir hayli zorlayıcıdır. Bu parçaların üretiminde yaygın olarak kullanılan geleneksel talaşlı imalat operasyonlarında, yüksek takım aşınması nedeniyle, tanımlanabilen kesme hızı dolayısıyla da talaş kaldırma hızı sınırlıdır. Yüksek kaliteli, düşük hazırlık zamanlı ve düşük maliyetli parça üretimine olan pazar talebinin artışı nedeniyle, kesilmesi zor malzemelerin yüksek verimlilikle talaşlı işlenebilmesi için alternatif tekniklere ihtiyaç duyulmaktadır. Son yıllarda artmaya devam eden yüksek iş mili devri, yüksek esneklik ve yüksek hassasiyet sağlayan tezgahlar sayesinde üretim kapasitelerinde de önemli artışlar mümkün hale gelmiştir. Bahsi geçen pazar talebine çözüm olarak sunulan çok eksenli talaşlı imalat operasyonları, başta havacılık ve savunma olmak üzere değişik sektörlerde hızla yaygınlaşmaya devam etmektedir. Genellikle çok maksatlı tezgahlar üzerinde gerçekleştirilen bu süreçlerde, aynı anda aynı parça birden fazla kesici ile eş zamanlı işlenebildiği gibi, iki ya da daha çok parça da eşzamanlı olarak işlenebilmektedir.

Geleneksel torna ve freze operasyonlarının aynı anda gerçekleştiği çok eksenli bir kesme süreci olan frezeyle tornalama operasyonu, Ti ve Ni alaşımları gibi kesilmesi zor malzemelerin yanında büyük çapları nedeniyle geleneksel torna tezgahlarında yüksek hızlarda döndürülemeyen işparçalarının yüksek verimlilikle işlenmesine de çözüm

sunmaktadır. Bununla birlikte frezeyle tornalama operasyonu ile ilgili literatür de bulunan kaynaklar sınırlıdır. Diğer taraftan, frezeyle tornalama operasyonlarının yüksek eksen esneklikleri ve kabiliyetleri nedeniyle, sürecin önerdiği avantajlardan tam anlamıyla yararlanmak için sistemde bulunan çok sayıda parametrenin uygun şekilde seçilmesi gerekmektedir. Bu durumun sağlanması için bütün süreç parametrelerini içeren süreç modellerine ihtiyaç duyulmaktadır. Bu tez kapsamında, frezeyle tornalama operasyonlarında süreç geometrisi, talaş oluşumu ve kesme kuvveti ile ilgili eksantriklik etkisini de kapsayan analitik modeller sunulmuştur. Ek olarak, yuvarlaklık, pürüz yüksekliği ve yüzey pürüzlülüğü modellenmiş ve benzetim çalışmaları gerçekleştirilmiştir. Analitik modeller ve deneysel tahminler çok maksatlı takım tezgahında farklı kesme koşullarında uygulanan deneyler ile doğrulanmıştır. Frezeyle tornalama sürecinin işlenmesi zor malzemeler üzerine olan etkisini saptamak için yapılan takım ömrü testleri de aynı takım tezgahında uygulanmıştır. Benzetim çalışmaları ve deneysel sonuçlar göstermektedir ki; operasyon şartları doğru bir biçimde seçildiği takdirde, frezeyle tornalama sürecinde kesimi zor malzemelerin işlenmesi sırasında üretim verimliliğinde önemli miktarda artış sağlanabilmektedir.

ACKNOWLEDGEMENTS

TABLE OF CONTENTS

LIST OF FIGURES

LIST OF TABLES

NOMENCLATURE

NC	Numeric Control
CNC	Computer Numeric Control
Ti	Titanium
Ni	Nickel
HSTM	High Speed Turn-Milling
R_a	Surface roughness
MQL	Minimum Quantity Lubricant
CAD	Computer Aided Design
CAM	Computer Aided Manufacturing
PMC	Polymer Matrix Composite
MMC	Metal Matrix Composite
CMC	Ceramic Matrix Composite
f_z	Feed per tooth
a_e	Feed per workpiece revolution
a_p	Axial depth of cut
e	Eccentricity
n_t	Rotational speed of tool
n_w	Rotational speed of workpiece
R_t	Radius of tool
R_w	Radius of workpiece
P_L	Projection length of tool onto workpiece
m	Number of cutting teeth
j	Index of tooth
r_n	Rotational speed ration of tool over workpiece
φ_{st}	Start angle of immersion
φ_{ex}	Exit angle of immersion
h	Chip height
V_c	Cutting speed
α	Rake angle
η_s	Shear flow angle
η_c	Chip flow angle
α_n	Normal rake angle

β	Friction angle
β_n	Normal friction angle
ϕ_s	Shear angle
K_{tc}, K_{rc}, K_{ac}	Cutting force coefficients
K_{te}, K_{re}, K_{ae}	Edge force coefficients
v_f	Feed speed
D_t	Diameter of tool
L_n	Minor cutting edge length of the tool insert
B_f	Feed mark angle
θ	Angle between facets
a_{ecrit}	Critical feed per workpiece revolution
$circ_{rough}$	Roughness in circumferential direction
ch	Cusp height
b_s1	Standard insert parallel land length
b_s2	Wiper insert parallel land length

CHAPTER 1

1. INTRODUCTION

In today's manufacturing environment, final shaped of most mechanical parts are produced by metal cutting methods. Similar to the other methods, then main goal is to achieve the fastest and most economical production with desired quality. The desired final geometry is generated by removing the unwanted material in the form of small chips by a cutting tool from the workpiece material which has lower hardness with respect to cutting tool. Machining is one of the oldest and most common types of manufacturing especially for metals, which is also the focus of this thesis. There are several metal cutting processes such as turning, milling, drilling, broaching, reaming, grinding and lapping, use of the first two ones are more common in industry due to their high versatility.

The machining is generally used by aerospace, defense, die and mold making, automotive, energy, medical products, electronics, micro systems industries. As far as the industries concerned, metal machining maintain to gain importance day by day.

An increase in potential production capacity was observed in the recent years due to improvements in machine tools which offer high precision, spindle speed, multi-axis flexibility. Multi-axis machining can be defined as the machining processes, where more than standard 3 axis: rotational and translational, are participated in the process. In 3 axis milling the cutting can have simultaneous translation x, y and z axis. On the other hand, simultaneous cutting operations on the same part or machining of more than one part simultaneously is performed on multi-tasking operations. Although the axis

flexibilities and capabilities are the same for two different multi-tasking machine tool, the configurations of them can be differ from each other based on the demands and expectations.

1.1. Multi-axis machining processes

Machine tools are the equipments whose fundamental functions are to transform raw materials with given mechanical properties to the finished parts within desirable geometry, dimensions and surface quality.

Modern machine tools were developed prior to during industrial revolution in 18th century. Initially, the boring machine and then lathe were used for a long time but later in order to increase productivity, the multi-axis turning machine tool was designed. This machine tool configuration enabled to do several turning operations on one machine simultaneously. With increasing demands and part complexities, the number of simultaneous axes control of turning center was increased. Figure 1-1 illustrates a history of the enhancements in the configuration of turning centers.
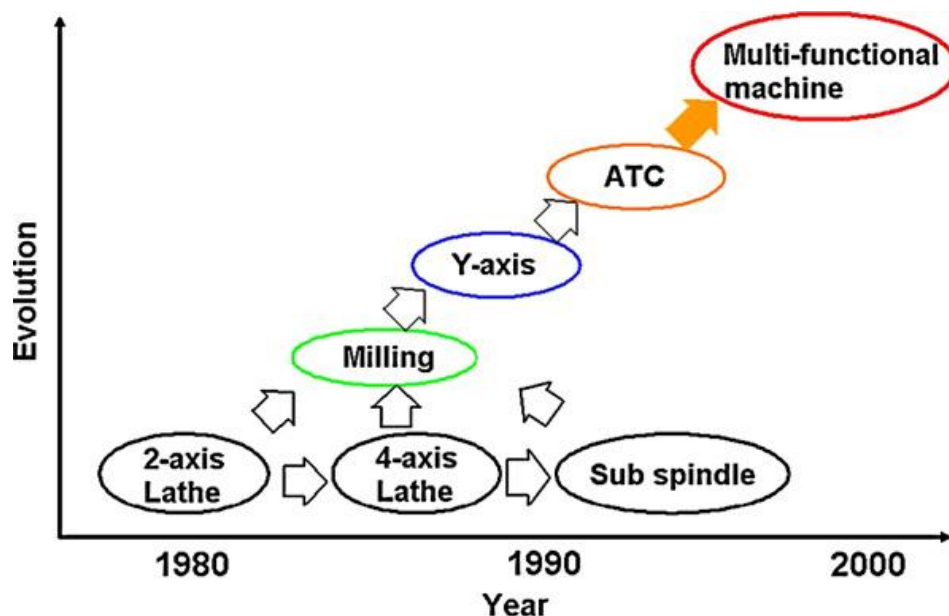
Figure 1-1: The evolution of turning machines [1]

Then first milling machine which was mainly used for machining of flat surfaces, was developed in 1827. Designing of machining center was a remarkable improvement of the NC milling machine in 1958 [1].
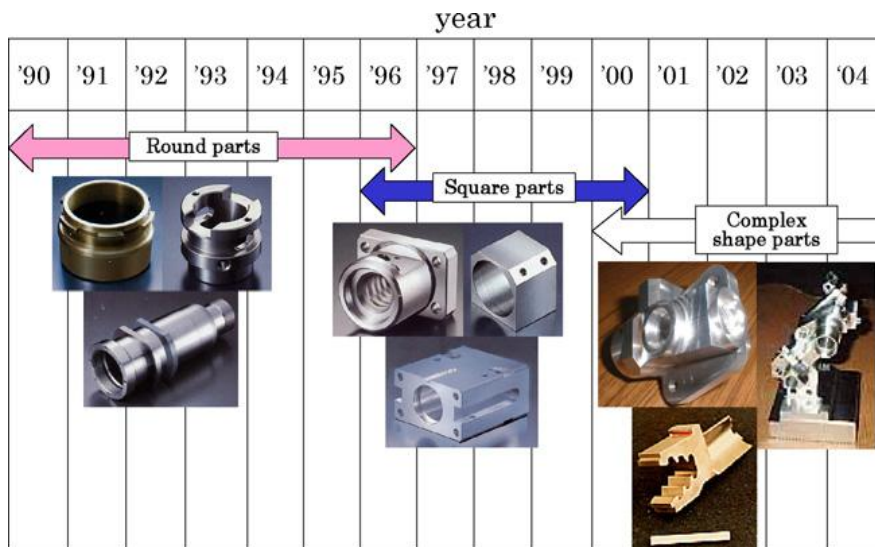
Figure 1-2: The evolution of parts machined by turning machines [1]

As demands are increasing to produce parts with strict tolerances at reduced cost, the processes are required to have higher machining accuracy and speed. Thanks to the developing technology, the requirements, which come from industry, are also increasing to machine difficult-to-cut materials and geometrically complex parts. In order to assure such requirements, the machine tools are expected to have multiple functions with reconfigurable design architectures [2][3][4].

Figure 1-3: Typical machining operations for multi-axis and parallel machine tools [5][6]

In opposition to performing required operations to a series of many single purpose machine tools, it is essential to have a machine tool which can perform several operations in order to produce complex parts with small quantity. Different types of multi-purpose machine tool with integrated processes have been created both general and specific conditions as shown in Figure 1-3 [7][8].

1.1.1. Turn-milling

Aerospace and defense industries are characterized by a high degree of research intensity and rapid developments. Because of this, corresponding industries have a high strategic importance in the development of innovative technologies. This gives new relevance for the research of new materials and processes. Turn-milling is a relatively new process which combines turning and milling operations can meet the requirements of aerospace and defense industries. As the growing of complexity of designed parts and increasing of turn-mill machine tools, turn-milling is gaining more and more application in these industries. Figure 1-4 shows the axis capability of a turn-milling machining center.
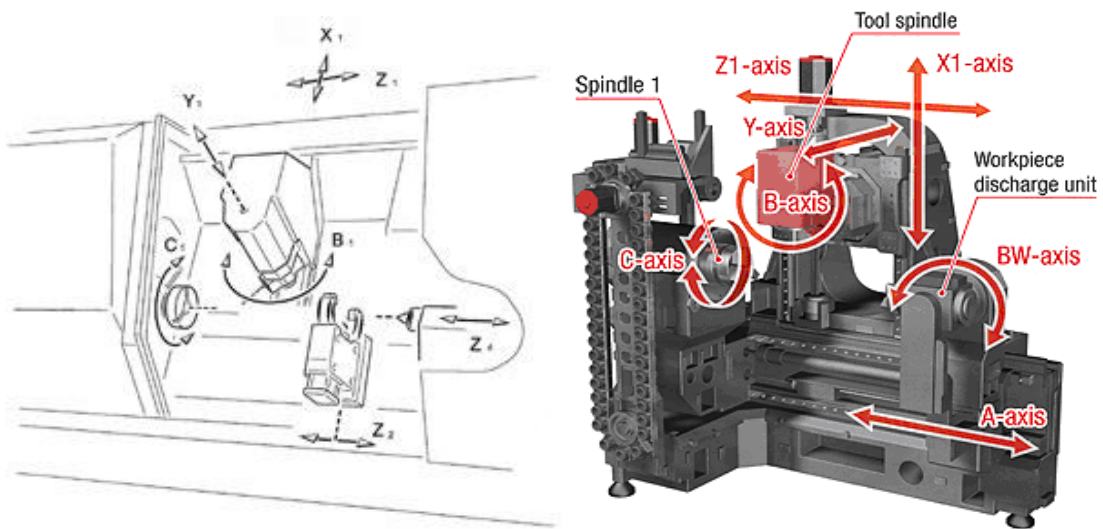
Figure 1-4: Axis representation in multi-purpose machine tool [5]

This relatively new technology offer increased productivity especially for difficult-to-machine materials such as Inconel 718, Ti6Al4V and Waspaloy which are called as high temperature alloys. In addition, turn-milling offer advantage for workpieces with large diameter which cannot be rotated at high speeds on conventional lathes. Different types of turn-milling operations are illustrated in Figure 1-5.
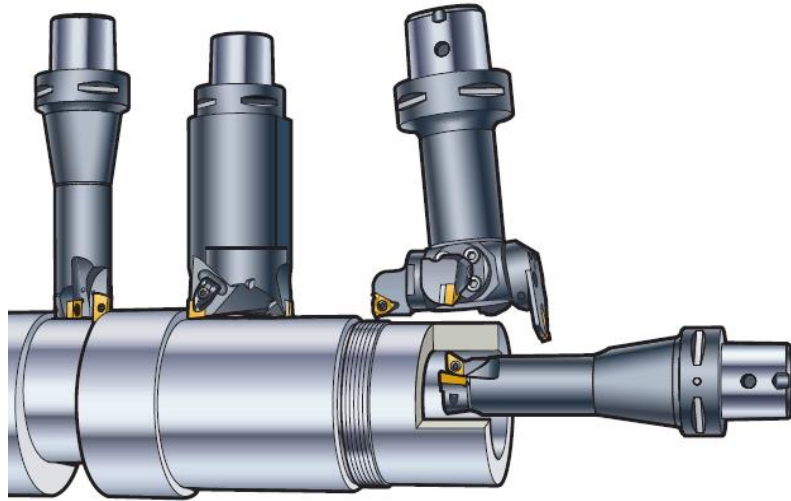
Figure 1-5: Examples for turn-milling operations [9]

Because of the ability move in multiple axis, over and above the conventional machines, turn-milling process is capable of producing highly complicated components with strict tolerances. At first glance, turn-milling machining centers seem a significant capital investment. However, their high ability to manufacture complex parts and high tolerance capability provide return on investment. Additionally, turn-milling offers many advantages especially about tool life which are discussed next sections. Figure 1-6 point outs typical machined parts produced by turn-milling operation.

Figure 1-6: Typical parts requiring turn-milling process [10][11]

5

Turn-milling process is classified into orthogonal turn-milling, tangential turn-milling and co-axial turn-milling. Although, all types are similar with regard to material removal rates and chip removal, the fundamental differences between this types ensue from only the tool geometry and the cutting kinematics.

1.1.1.1.   Orthogonal turn-milling

As can be observed from the Figure 1-7, orthogonal turn-milling is a widely used turn-milling process in which the axis of the cutting tool and the workpiece are perpendicular to the each other [12]. The chip is generated by both side and bottom edges of the cutting tool [13]. Orthogonal turn-milling is suitable for external machining of rotationally symmetrical workpieces. In addition, this process can be performed as longitudinal or plunge with respect to feed rate direction of the cutting tool. Orthogonal turn-milling will be investigated analytically and experimentally through this thesis.
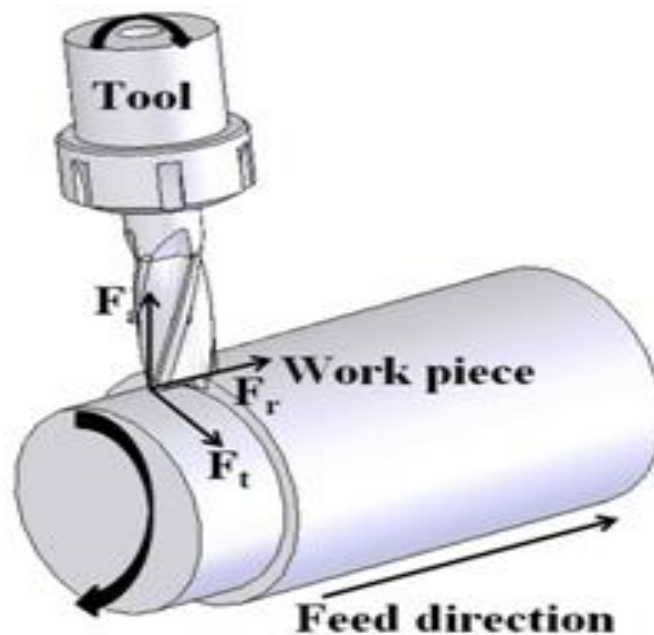
Figure 1-7: Orthogonal turn-milling operation

1.1.1.1.1.   Eccentricity

Due to the multi-axis flexibility of the turn-milling processes, eccentricity which means axis offset in Y direction, can be defined in orthogonal turn-milling operations. Eccentricity, which is one of the main focuses of this thesis and will be investigated in the following sections in detail, influences almost all of the process parameters and offers various advantages. As an example, the maximum feed rate can be defined up to

the length of the projection of the minor cutting edge onto workpiece in orthogonal turn-milling. If feed rate is defined over than that length, cutting tool left behind uncut surface. On the other hand, by using eccentricity parameter which is shown in Figure 1-8, maximum feed rate in other words productivity can be increased without sacrificing surface quality.
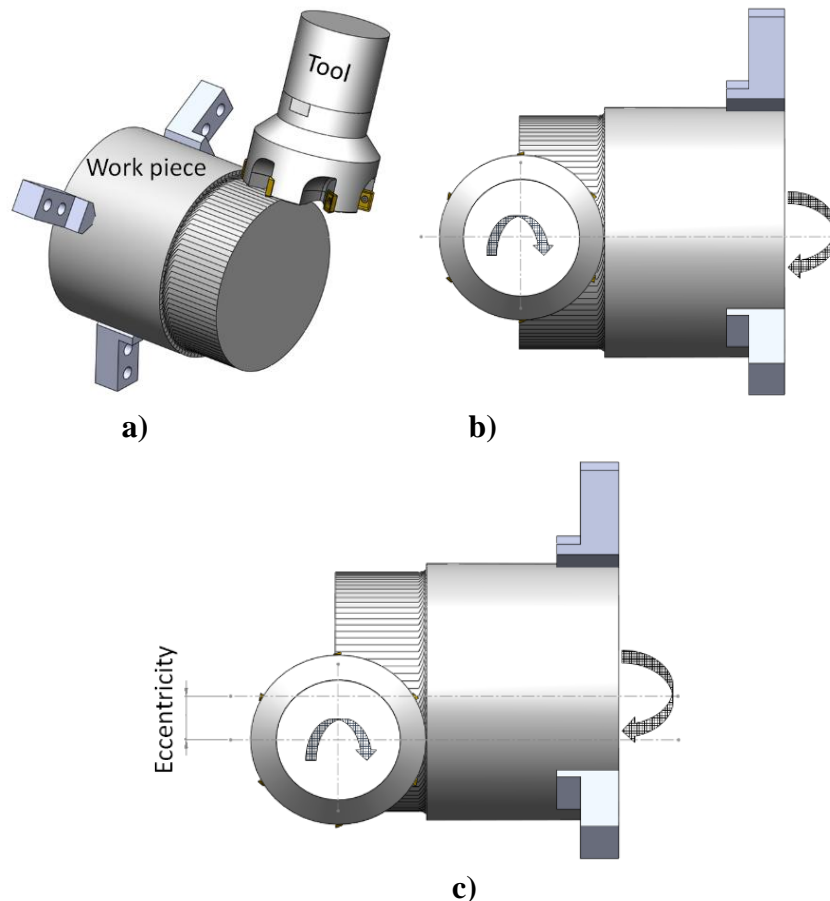
Figure 1-8: a) 3D, b) centric (eccentricity=0) and c) eccentric (e>0) representations of orthogonal turn-milling

1.1.1.2. Tangential turn-milling

As shown in Figure 1-9, tangential turn-milling is a multi-axis machining operation in which cutting tool is tangent to the workpiece. As opposed to the orthogonal turn-milling, the chip is only formed by the side edges of the cutting tool.
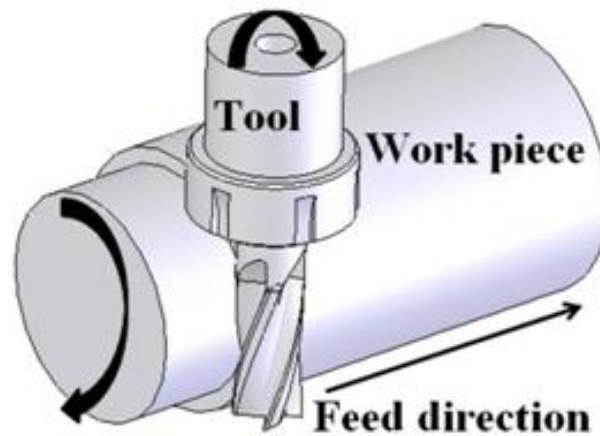
Figure 1-9: Tangential turn-milling operation

1.1.1.3.   Co-axial turn-milling

As illustrated in Figure 1-10, co-axial turn-milling is a type of turn-milling process in which the axis of the cutting tool and the workpiece are parallel to each other. As a result of this, only side edges of the cutting tool involve in machining operation. Co-axial turn-milling can be used internal as well as external machining of rotationally symmetrical workpieces.
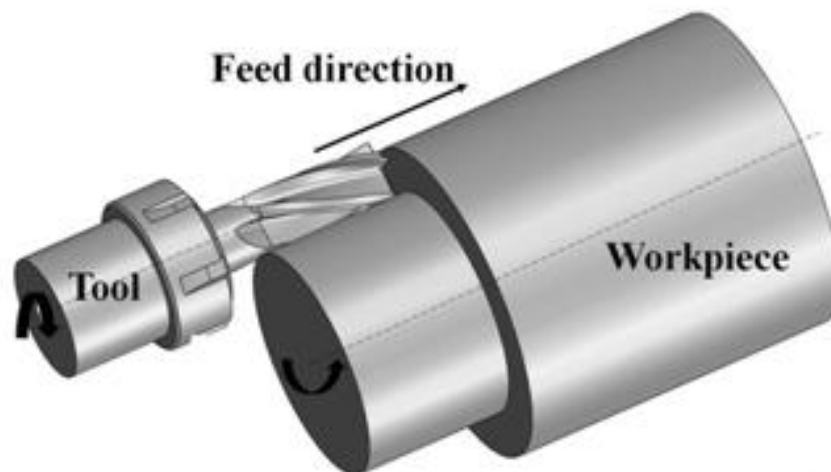
Figure 1-10: Co-axial turn-milling operation

1.2. Literature survey

The previous studies related to proposed contributions of this thesis are summarized in this section. General outline of turn-milling process related researches are presented. This study focuses on the mechanics of the orthogonal turn-milling process. However, process geometry affects mechanics of the process. Because of that reason, before going into details about the process mechanics, the process geometry required to be explained

well. After that, simulation and modeling of cutting force related studies are reviewed. In order to calculate process forces, chip formation and engagement boundaries of tool and workpiece should be defined. Moreover, corresponding definitions can help to interpret engagement related phenomenon. Because of this reason, related literature about surface quality, material removal rate and tool life are represented respectively.

First academic studies related to turn-milling have started in 1990 by Schulz and Spur [15]. Based on the cutting tool and workpiece positions, they classified turn-milling processes as orthogonal and co-axial. In this study, chip geometry, geometric accuracy and eccentricity are investigated for orthogonal turn-milling operations. Moreover, they turn-milled plain bearing half liners which are generally machined by internal turning. They expressed that performing high speed turn-milling (HSTM) with high surface quality and low thermal stress on the cutting edge is possible.

Researches about turn-milling process forces were done first by Filho [13]. He conducted a series of orthogonal turn-milling experiments on a five axis machining center, measured cutting forces and compared them with analytical model predictions for plunge type centric orthogonal turn-milling. In a later study, Karagüzel et al. [16] developed process models for orthogonal, tangential and co-axial turn-milling operations. Thus, for the first time in literature engagement limits and uncut chip geometry were introduced for three types of turn-milling operation. Moreover, as an original contribution to the literature, cutting forces were calculated by using orthogonal to oblique transformation. They also verified their models with experiments for different cutting conditions. Process forces concerning the eccentricity effect were first investigated by Karagüzel et al. [17]. They found from analytical models and verified with experiments that cutting forces decreased with increasing eccentricity. In this study, the models expressed for tool and workpiece engagement length changes with respect to eccentricity parameter also help to understand tool life studies. In a recent work, Qui et al. [18] introduced an approach for prediction of cutting forces in orthogonal turn-milling with round inserts. They determined the engagement cutting region by using mapping method.

Researchers have generally focused on dimensional accuracy and surface quality of finished product. One of the early works related to this topic for brass and mild steel under specified speeds and feeds was done by Choudhury and Mangrulkar [19]. Surface roughness data operation, obtained from orthogonal turn-milling operation by using

vertical milling machine, were compared with ones obtained from conventional turning operation. They deduced that orthogonal turn-milling provided 10 times better surface quality compared to conventional turning. In another study, Choudhury and Bajpai [12] investigated again the surface quality in orthogonal turn-milling. The main difference from the previous research is that this time they compared the obtained results with ones obtained from conventional milling. In this research, It has been shown that surface quality obtained by orthogonal turn-milling process is higher than that of conventional milling process for mild-steel workpiece. Another study based on surface generation was done by Zhu et al. [20] who proposed two mathematical models which identify surface roughness and topography in orthogonal turn-milling. They conducted various experiments to verify their models and presented some parameter selection criteria based on theoretical and experimental results. Savaş et al. [21] investigated the surface roughness in tangential turn-milling for different depth of cuts, feeds and cutting speeds experimentally. They declared that really good surface quality was obtained which is comparable to grinding operation. According to them, tangential turn-milling can replace grinding process.

One of the most important parameters is eccentricity which is a special parameter for orthogonal turn-milling. Furthermore, investigation of the effects of eccentricity on different parameters is main focus of this thesis. Kopac et al. [22] researched the effect of eccentricity on surface quality in turn-milling and tried to find an optimum eccentricity for better surface finish. They reported that surface roughness R_a in alongside direction in eccentric turn-milling is much better than that the one in centric turn-milling. In another study, geometric surface roughness model is developed in order to analyze the effect of cutting parameters by Yuan and Zheng [23]. Their models were included cutter radius, feed, cutting speed, number of teeth and eccentricity. In a recent study, Uysal et al. [24] demonstrated the eccentricity effects on turn-milling process parameters such as chip formation, circumferential and alongside surface roughness, productivity and tool wear. They proposed analytical models and verified them with experiments.

In addition to surface roughness studies, researchers were also investigated the productivity which is one of the main advantages of turn-milling. Neagu et al. [25] examined the kinematics of orthogonal turn-milling regarding to cutting speed, roundness and tool geometry. They stated that with turn-milling process, it is possible to

obtain twentyfold higher material removal rate compared to traditional turning process for a rough machining operation.

Turn-milling is a relatively new operation which contains turning and milling processes and offer remarkable advantages because of its interrupted cutting characteristics. This phenomenon contributes to maintain lower cutting temperatures [9]. Stephenson and Ali [26] emphasized that under the same cutting conditions, the temperatures are lower in intermittent cutting than those in continuous cutting. For that reason, intermittent characteristics of turn-milling helps maintaining lower cutting temperatures which enable to define higher cutting speeds, produce smaller chips and reduce cutting forces.

In contrast with continuously cutting operations, interrupted cutting reduces the contact time per tooth and respites of cutter to cool down which helps to increase tool life. As a result, turn-milling can offer higher productivity especially for difficult-to-cut materials [27][28].

Because of their low machinability and red hardness, machining of difficult-to-cut materials is challenging. Titanium and nickel based alloys are the most popular examples for these materials. Increase in demands for high strength-to weight ratio materials result in use of more super alloys in special applications such as jet engine components [29][30]. Although obtained cutting temperatures in turn-milling is lower than those obtained in conventional turning, machining of difficult-to-cut materials is still problematic because of their low thermal conductivity and high heat resistance [31].

In literature, there are some applications for improved tool life while machining of corresponding materials. Cooling strategies such as minimum quantity lubrication (MQL) [32], cryogenic machining [33] and high pressure flood cooling [34] can be given as an example. Moreover, cooling strategies also helps to remove chips from cutting zone. In a recent study, Karagüzel et al. [35] examined the cooling strategies and cutting process effects on tool wear for hard to machine materials. They conducted tool wear experiments in turn-milling, rotary turning, which is another multi-axis machining operation, and conventional turning for flood coolant, MQL and dry cutting conditions. Taking into consideration each material, tool life results for turn-milling is always better than both rotary turning and conventional turning ones. Additionally, they reported that for Ti6Al4V machining 25 times longer tool life is obtained compared to conventional turning operation under same cutting conditions. Pogacnik and Kopac [36] studied the

effect of entry and exit conditions on tool life showing that they are very important in order to determine the optimum cutting condition. They declared that the superiority of turn-milling over conventional turning become more obvious at higher cutting speed.

1.3. Objective

Decision on process parameter selection is extremely important to detect prospective problems. In industrial applications, corresponding parameters selected based on trial and error method or process planner's experiences. Because of the iterations in the trial and error method, occupy rather process equipment availability that's why this is not a convenient approach.

As discussed in previous section, various models and approximations are reviewed. The modeling of cutting operation is required for the selection of optimum cutting parameters for the industrial applications, and for the research of the cutting process for the scientists.

The main motivation behind this thesis is to meet the necessities for assistance in process planning for orthogonal turn-milling operations through proposed guidelines based on process modeling and simulation. The effect of process parameters on the cutting forces and form errors can be predicted. Process planner determines the process parameters according to the prediction of the process models by avoiding iterations on the real set-up. Hence, the potential problems can be eliminated before the actual machining operation which saves considerable amount of time and cost. In addition to the process models, this thesis is also concentrated on the tool life of the difficult-to-cut materials in turn-milling processes for different cutting conditions.

1.4. Organization of the thesis

The thesis is organized as follows;

After this introductory section, experimental procedures of cutting tests are introduced with machine tools, workpiece materials, cutting tools and measurement equipments in Chapter 2.

In Chapter 3, cutting forces in orthogonal turn-milling operation including eccentricity effect are modeled by using semi-analytical approach. Simulation results are verified with experimental ones for different cutting conditions.

In chapter 4, circularity, cusp height and circumferential surface roughness which are the main surface form errors, are analytically modeled and validated with experiments by considering different cutting conditions. Parameter selection criteria for optimum material removal rate are proposed. The effect of wiper insert on surface generation is also investigated experimentally.

In chapter 5, experimental results of tool life tests are presented for different difficult-to-machine materials and cutting conditions. In order to detect the promised superiority of turn-milling over traditional processes, the obtained results for turn-milling are compared with the ones obtained from conventional turning. Additionally, the effect of eccentricity and inclination angle on tool life are also investigated.

Suggestions for future research are expressed in chapter 6. Additionally, conclusions and discussions are presented in chapter 7.

1.5. Summary

In this chapter, an introduction for multi-axis machining and orthogonal turn-milling by considering different types of the operation are given. Although, the work done on this type of operation is limited, an overview of researches on modeling of process geometry, mechanics and machining parameter selection and optimization for orthogonal turn-milling is presented.

.

CHAPTER 2

2. EXPERIMENTAL PROCEDURE

In this thesis, orthogonal turn-milling operations are investigated from cutting force, surface form errors and tool life point of views. The cutting tests were conducted on a wide range of cutting conditions in order to obtain better and various data. In order to express the superiority of the multi-purpose machining operations over traditional ones, tool life tests were implemented on two different machining processes, conventional turning and turn-milling. These tests were applied for different testing materials especially difficult to cut materials and performed on conventional turning operation with the same cutting conditions in order to emphasize the importance of the orthogonal turn-milling process.

In this section, used machine tools, workpiece materials, cutting tools, measurement and data acquisition equipments and coolant strategies throughout the study are introduced.

2.1. Workpiece Materials

Recently, starting with the industrial demands and challenges, demands for super alloys have been increasing in applications requiring high performance. Figure 2-1 represents the strength of special materials with respect to working temperatures. These materials are commonly used in aerospace and defense industries because of their high strength/weight ratio even at elevated temperatures.
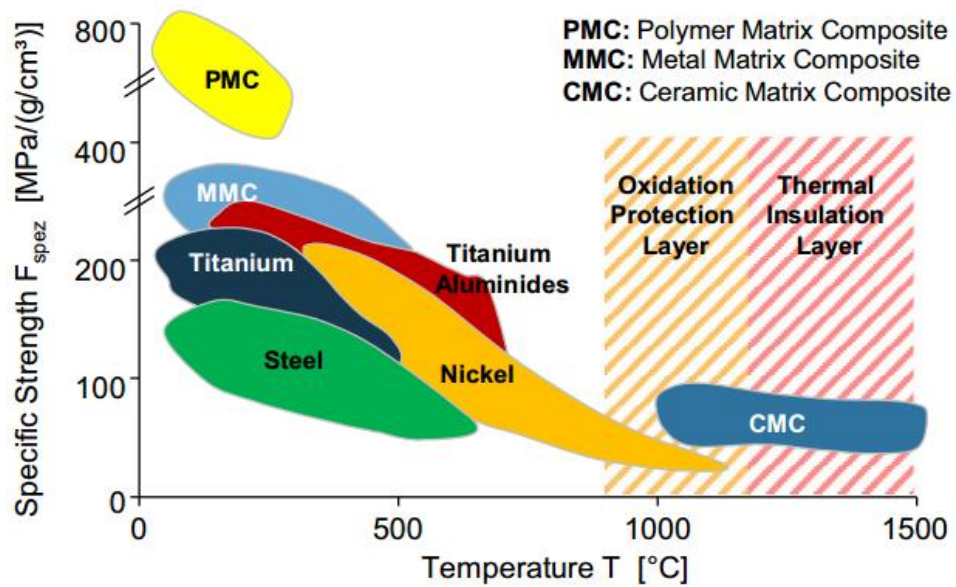
Figure 2-1: Specific strength of materials with respect to working temperature [37]

Figure 2-2 illustrates the cross section of jet engine which is one of the main usage fields of specific materials.
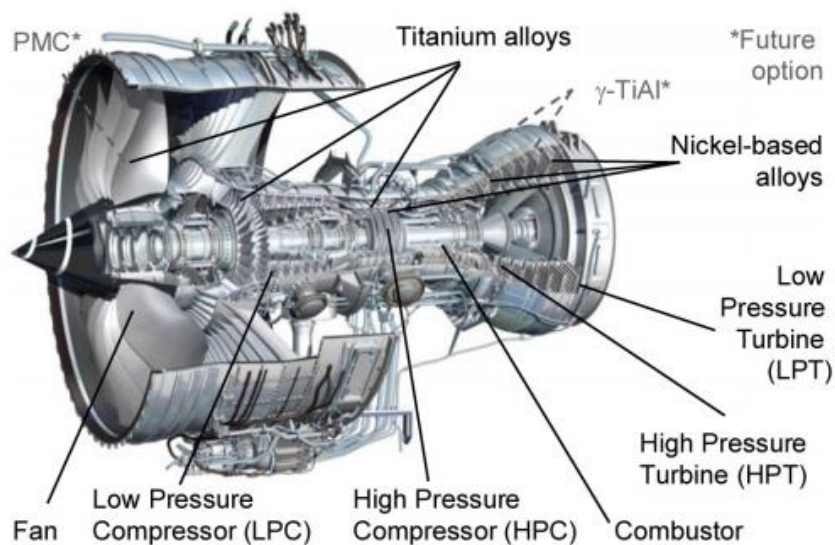
Figure 2-2: Current and future temperature specific materials in jet engine [38]

Due to low productivity, diminished geometrical accuracy, high cutting forces, increased tool wear and high tool expenses, machining of difficult-to-cut materials using conventional operations are extremely challenging. On the other hand, turn-milling operations can be remedy for these problems.

2.1.1. AISI 1050 Steel

Although AISI 1050 steel is not a super alloy, it was used for investigating eccentricity effect both on tool life and surface roughness. Additionally, it was used for verification of cutting force and form error models. This material is one of the most economical grades of the heat annealed spring steel and is very commonly preferred in manufacturing. The metallurgical properties of AISI 1050 steel are given in Table 2-1.

Table 2-1: Metallurgical properties of AISI 1050 steel

Element	C	Mn	P	S	Fe
Content (%)	0.51	0.75	0.04	0.05	Balance

Mechanical and thermal properties of AISI 1050 steel whose density is 7800kg/m^3 are given in Table 2-2.

Table 2-2: Mechanical and thermal properties of AISI 1050 steel

Property	Value [Metric]
Tensile Strength	636 MPa
Yield Strength	365.4 MPa
Elasticity Modulus	195 GPa
Shear Modulus	80 GPa
Poisson's Ratio	0.28
Brinell Hardness	187 HB
Impact Strength	16.9 J
Elongation	23.7 %
Reduction in Area	39 %
Specific Heat Capacity	450J/kg*K
Thermal Conductivity	49.5 W/m*K

2.1.2. Inconel 718

Inconel 718 is thermal-resistant austenitic nickel based super alloy, used in a wide range of applications. This material retains excellent mechanical and chemical properties even

at high temperatures which is called red hardness. This characteristic cause poor machinability thus, the problem of machining Inconel 718 is one of ever-increasing interest. The metallurgical properties of Inconel 718 are given in

Table 2-3.

Table 2-3: Metallurgical properties of Inconel 718

Element	C	Mn	Si	Cr	Ni	Co	Mo	Nb+Ta	Fe	Ti	Al	Cu
Content (%)	0.030	0.16	0.11	18.10	Balance	0.37	3.04	5.34	18.26	0.98	0.49	0.10

Because of its good corrosion and oxidation resistance even at elevated temperature, Inconel 718 is widely used in nuclear power plants and oil gas industries. Mechanical and thermal properties of corresponding material whose density is 8190kg/m^3 are illustrated in Table 2-4.

Table 2-4: Mechanical and thermal properties of Inconel 718

Property	Value [Metric]
Tensile Strength	1365 MPa
Yield Strength	1034 MPa
Elasticity Modulus	206 GPa
Shear Modulus	100 GPa
Poisson's Ratio	0.26
Brinell Hardness	331 HB
Elongation	12 %
Reduction in Area	15 %
Specific Heat Capacity	435 J/kg*K
Thermal Conductivity	11.4 W/m*K
Melting Temperature	1265 °C

2.1.3. Waspaloy

Waspaloy, registered trademark of United Technologies Corporation, is nickel-base, age hardenable super alloy with excellent high temperature strength and good corrosion

resistance even at elevated temperatures. This material is mostly used in aircraft turbine engines and compressor disk. Historically, one drawback of super alloys has been their poor machinability. This is where the importance of turn-milling comes in. The metallurgical properties of Waspaloy are given in Table 2-5.

Table 2-5: Metallurgical properties of Waspaloy

Element	C	Mn	Si	Cr	Ni	Co	Mo	Zr	Fe	Ti	Al
Content (%)	0.062	0.02	0.10	19.35	Balance	13.34	4.19	0.062	0.82	2.94	1.30

Mechanical and thermal properties of Waspaloy whose density is 8190kg/m^3 are shown in Table 2-6.

Table 2-6: Mechanical and thermal properties of Waspaloy

Property	Value [Metric]
Tensile Strength	1315MPa
Yield Strength	910 MPa
Elasticity Modulus	211 GPa
Poisson's Ratio	0.29
Brinell Hardness	351 HB
Elongation	26 %
Reduction in Area	25 %
Specific Heat Capacity	461 J/kg*K
Thermal Conductivity	12.6 W/m*K
Melting Point	1335 °C

2.1.4. Ti6Al4V

Ti6Al4V is the most widely used titanium alloy. The Ti6Al4V alloy offers high performance for a variety of weight reduction applications in aerospace, automotive and marine equipment industries because of its high strength/weight ratio. It is significantly stronger than commercially pure titanium while having the same stiffness and thermal properties. The metallurgical properties of Ti6Al4V are given in Table 2-7.

Table 2-7: Metallurgical properties of Ti6Al4V

Element	C	V	Si	H	N	O	Fe	Ti	Al	Ti
Content (%)	0.07	4.2	0.15	0.015	0.05	0.15	0.23	Balance	5.9	Balance

Among its many advantages, it is heat treatable and has an excellent combination of strength and corrosion resistance. Mechanical and thermal properties of Ti6Al4V whose density is 4430kg/m^3 are given in Table 2-8.

Table 2-8: Mechanical and thermal properties of Ti6Al4V

Property	Value [Metric]
Tensile Strength	950 MPa
Yield Strength	875 MPa
Elasticity Modulus	115 GPa
Shear Modulus	60 GPa
Poisson's Ratio	0.33
Brinell Hardness	291 HB
Elongation	13 %
Reduction in Area	34%
Specific Heat Capacity	526 J/kg*K
Thermal Conductivity	6.7 W/m*K
Melting Point	1649 °C

2.2. Cutting Conditions

Tool life experiments were implemented under dry, flood cooling and MQL conditions. In order to increase the tool life of cutting tools especially in machining of difficult-to-cut materials, cutting fluids are needed. In Section 5, the three types of coolant environments will be compared for difficult-to-cut materials machining. Cutting fluids are employed in machining operations to enhance the tribological mechanisms, which occur when two surfaces contact with each other. The cutting fluid improves the tool

life and surface conditions of the workpiece. It also contributes to remove the heat from machining area and produced chip during machining [39].

<p align="center">a)</p>
<p align="right">b)</p>

<p align="center">c)</p>
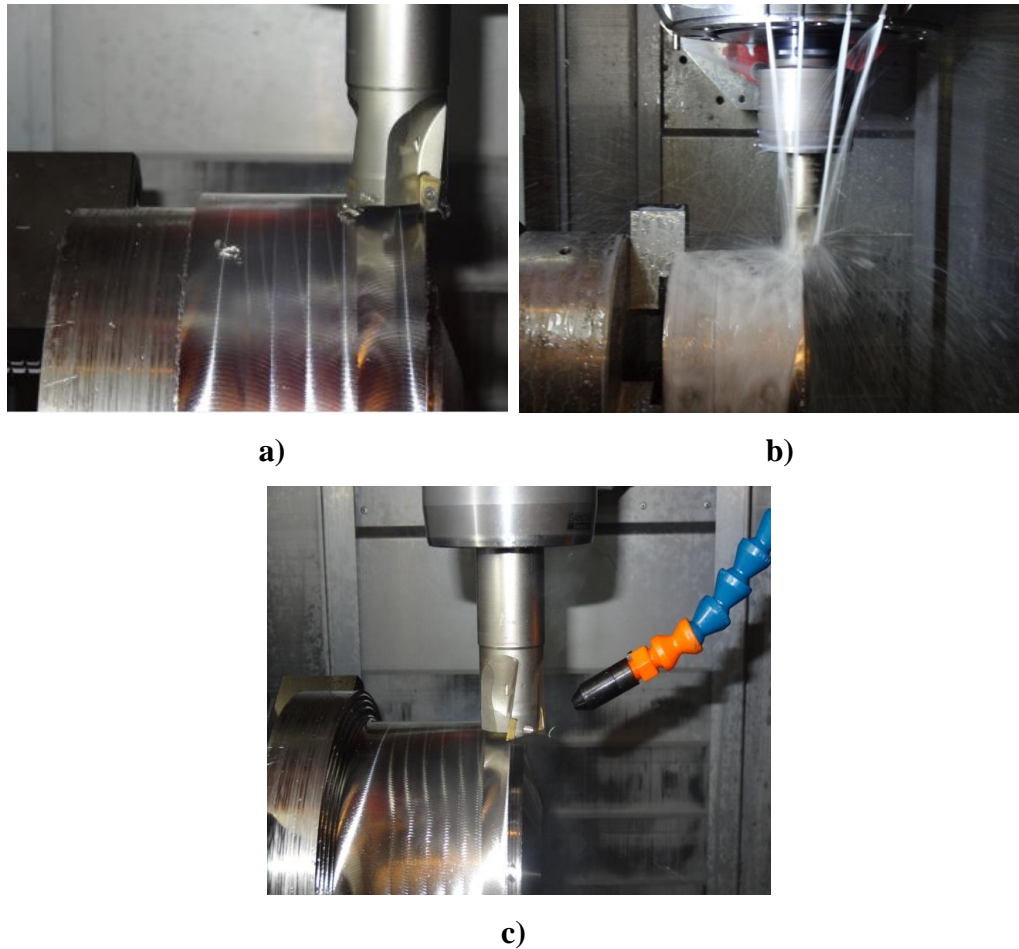
Figure 2-3: a) Dry, b) Flood and c) MQL coolant conditions in turn-milling

In the experiments WERTE MQL system was provided from an external nozzle at the cutting zone where Hard-Cut 5518 was preferred as the lubricant. Moreover, the system was operated at a pressure of 6 bars and a flow rate of 17mL/hour as shown in Figure 2-3a. In flood cooling experiments, Cool Rite 2290 (Long Life Coolant Soluble Oil) with a volume percentage of 5% was applied to the cutting regime as it can be seen in Figure 2-3b.

2.3. Machine Tools

Conventional turning processes were implemented on Mori Seiki NL1500 CNC lathe as illustrated in Figure 2-4. It is a 3 axes turning center with 6000rpm maximum spindle speed. Parts can be machined which has maximum 386mm diameter and 515mm length on this machine tool.

Figure 2-4: Mori Seiki NL1500 CNC Lathe

Almost all of the turn-milling tests and measurements were conducted on Mori Seiki NTX2000 Mill-Turn center as represented in Figure 2-5. This machine tool capable 9 axes movement with two chucks, a milling spindle and a turning turret. In addition to turn-milling, parallel turning and parallel milling operations can be done on this machine tool. Milling spindle can move along X, Y, Z axes and rotate around B axis. The machine tool has a maximum capacity of 61mm diameter and 1540mm workpiece length. Moreover, maximum spindle speed is 5000rpm and maximum tool spindle speed is 12000rpm.

Figure 2-5: Mori Seiki NTX2000 Mill-Turn Center

Cutting force model verification tests were implemented on DMG 50 Evo 5 axes machining center, which has 18000rpm maximum spindle speed, as shown in Figure 2-6. This machine tool have *X, Y, Z* linear and *B, C* rotational axes.

Figure 2-6: DMG 50 Evoluation 5 Axes Machining Center

2.4. Cutting Tools

Seco 32 mm diameter end mill tool, which has 20800rpm rotational speed limit, is shown in Figure 2-7a. This cutting tool was used for tool life tests of difficult-to-cut materials such as Waspaloy, Inconel 718 and Ti6Al4V. In addition, Seco 50mm diameter face mill tool, which has 14800rpm rotational speed limit, was used for determination of eccentricity effect and material removal rate tests as illustrated in Figure 2-7b.

a)   **b)**

Figure 2-7: Seco a) R217.69-3232.0-10-3A b) R220.53-0050-12-4A cutting tools

Sandvik Coromat 16mm diameter end mill tool, which has 41500rpm rotational speed limit, was used for verification of cutting force model tests as represented in Figure

2-8a. Moreover, Sandvik Coromat 50mm diameter face mill tool, which has 8900rpm rotational speed limit, was used for determination of eccentricity effect on material removal rate and tool life as shown in Figure 2-8b. Although Seco and Sandvik Coromat 50mm diameter face mill tools seems the same, their side edge cutting angles are different, thus they were used for different applications.

a)　　　　　　　　　　　　　　b)

Figure 2-8: Sandvik Coromat a) R390-016A16-11L b) R220.69-0050-18-4A cutting tools

In all cases, proper inserts were selected. Whereas MP2500 inserts were used for AISI 1050 steel, F40M inserts were used for Waspaloy, Inconel 718 and Ti6Al4V machining. Moreover, wiper inserts were used in surface roughness measurements as a special case.

2.5. Measuring Equipments

Turn-milling cutting forces were measured by using Kistler 9123C1111 rotating multi-component dynamometer as shown in Figure 2-9. The forces were measured in different cutting conditions and data were collected by using LabView software.

Figure 2-9: a) Kistler Rotating Multi-component Dynamometer (Type 9123C1111) b) Kistler Multichannel signal conditioner (Type 5223)

Nano Focus µSurf 3D profilometer was used in order to determine tool wear as illustrated in Figure 2-10. Cutting inserts were inspected at regular time intervals.
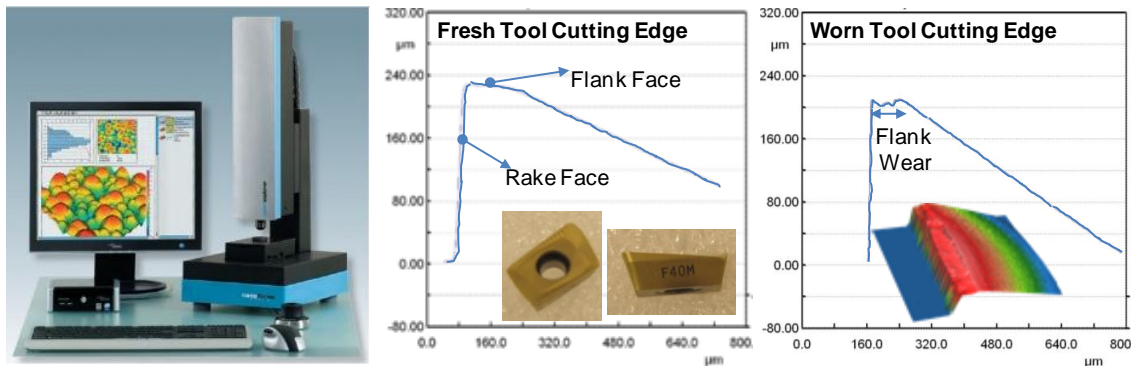
Figure 2-10: Nano Focus µSurf Non-Contact 3D Profilometer

Mitutoyo SJ 301 portable profilometer was used for surface roughness measurement in alongside direction as illustrated in Figure 2-11a. In addition, cusp height model verification tests were applied by using DIGI-MET Helios Preisser 1726502 as shown in Figure 2-11b.

a)   **b)**

Figure 2-11: a) Mitutoyo SJ 301 b) DIGI-MET Helios Preisser 1726502

2.6. Summary

In this chapter, details about experimental procedure of cutting tests by considering cutting tools, machine tools and measurement and data acquisition equipments are explained. Metallurgical, mechanical and thermal properties of machined workpieces are expressed in detail. In addition, selected coolant conditions which are used in tool life experiments, are expressed in detail.

CHAPTER 3

3. MODELING OF PROCESS FORCES

Prediction of cutting forces is a key factor in order to determine the process limitations. If cutting forces reach high values, resulting tool deflections may cause undesirable form errors. Additionally, because of the excessive stress as well as spindle overload, excessive cutting forces may lead to tool breakage. Prediction of cutting force methods are also necessary to optimize the process planning in CAD/CAM. Hence, modeling of cutting forces in turn-milling applications has an important role for selection of process parameters and cutting conditions.

In former studies, average rigid cutting force model [40], which asserts that the consumed average power, torque and tangential cutting force are directly proportional to the material removal rate, is used. Although, there are some other approximations based on material removal rate and cutting force relation, there is no direct relationship between cutting forces and material removal rate for milling operations.

Subsequently, it was realized that more detailed force models, which includes cutting tool and properties of workpiece materials, are required in order to predict the cutting force accurately. In milling processes, rake angle, oblique angle (helix angle), hone radius, insert edge radius and number of cutting tooth can be measured and implemented on cutting force model directly. Nowadays, cutting tool manufacturers can supply this detailed information or these properties can be measured under specified devices.

In this section, semi-analytical force model for orthogonal turn-milling operation is presented. First, fundamental properties for chip formation are determined. Chip formation models will also be helpful for stability analysis in future. Because of the variations in the cutting tool geometries, there are several force models for milling processes. In literature, empirical, semi-analytical and analytical models are the main types of these models which were done for conventional processes. Cutting force and edge force coefficients are determined by using mechanics of milling method [41]. In this method, cutting force coefficients are obtained from orthogonal database. In addition, shear angle, friction angle and shear stress parameters are also required for the cutting force calculation. The orthogonal databases consist of different feed rates, cutting speeds and rake angles for each tool workpiece material pair. In case, one of these components are changed, the orthogonal database test has to be repeated.

3.1. Uncut Chip Formation

By contrast with conventional processes, chip formation in turn-milling is obtained from simultaneous rotations of both cutting tool and workpiece. Due to the various process parameters, analytical modeling of chip formation is more complicated than conventional processes. As circumferential and axial there are two different feed rates in operation. Axial feed is the motion of cutting tool through the alongside direction of workpiece. On the other side, as a result of the simultaneous workpiece rotation, circumferential feed rate is identified as tool rotational motion around the workpiece. The combination of these two feed rates causes helical tool path as illustrated in Figure 3-1.
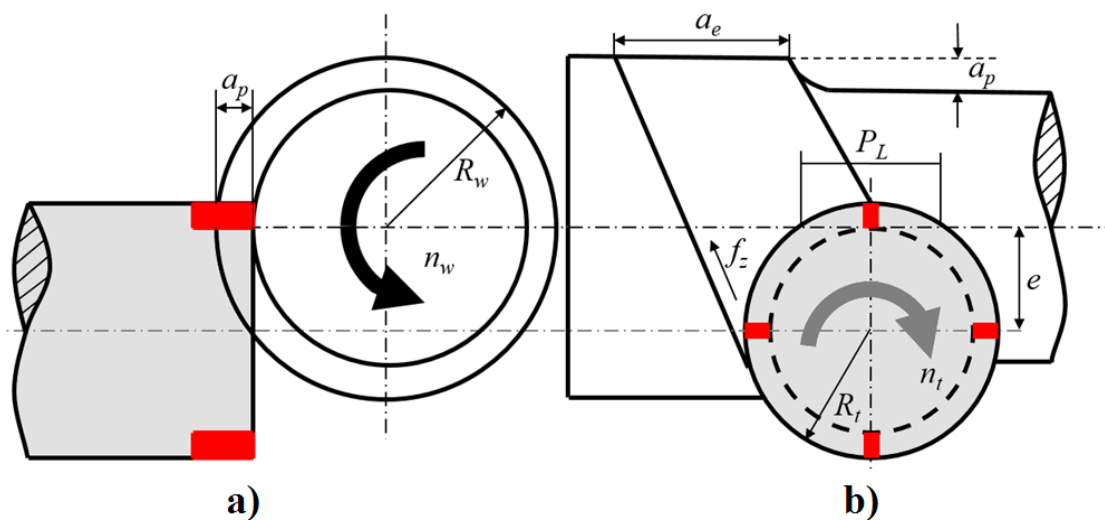
Figure 3-1: Process geometry in turn-milling a) Side view, b) Top view

Turn-milling process parameters are shown in Figure 3-1 which represents feed per tooth (f_z), feed per workpiece revolution (a_e), axial depth of cut (a_p), eccentricity (e), rotational speed of tool (n_t), rotational speed of workpiece (n_w), radius of tool (R_t), radius of workpiece (R_w), projection length of tool onto workpiece (P_L). Although some of the turn-mill process parameters seem new, they have same analogy with conventional milling and turning parameters. As an example, feed per workpiece revolution (a_e) has the same definition with radial depth of cut in conventional milling process. Moreover, circumferential feed rate (f_z) can be thought as feed rate in conventional milling operation. Chip is generated by both bottom and side edges of cutting tool in orthogonal turn-milling [13], in which workpiece and cutting tool rotational symmetry axis are perpendicular to the each other [12], as illustrated in Figure 3-2a. The main problem about modeling of cutting forces in orthogonal turn-milling is that the prediction of uncut chip formation because of it's strong dependence on eccentricity parameter. Three different cases for chip formation are observed due to the eccentricity. In Figure 3-2b represents the uncut chip formation within one tool revolution for a half immersion cutting. Moreover, the blue segments refer the instant chip cross section during operation.
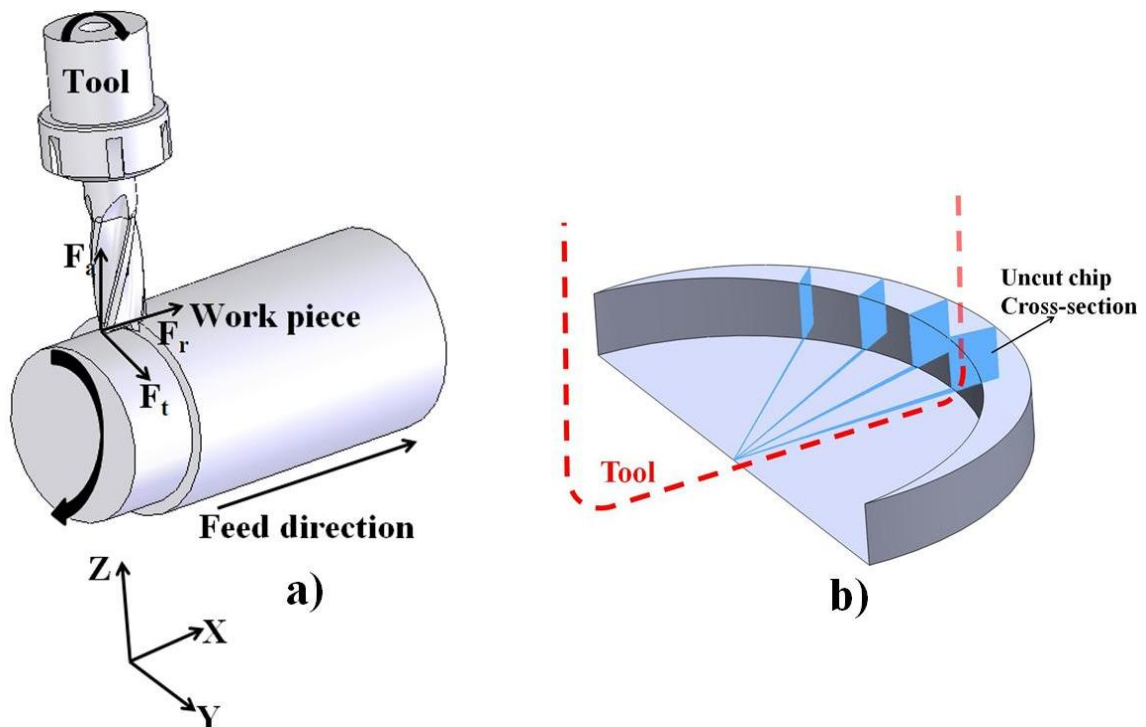
Figure 3-2: a) Tool-workpiece configuration and b) uncut chip geometry in orthogonal turn-milling

3.1.1. Centric Condition

Uncut chip formation segmentation for centric condition, which means eccentricity equals to zero, is shown in Figure 3-3. Based on the figure, while points 1, 2 and 2' represent the boundaries of previous position of the cutting tool, points 1, 3 and 3' represent the boundaries of current position of cutting tool. There are two different chip cross section area which are generated by bottom edge and side edge of the cutting tool. Angle θ is illustrated in Figure 3-3, represents the angle between line 1-2 and 1-3. It should be noted that corresponding angle also equals to facet angle which will be defined between subsequent facet middle points in Section 4.2.1 Thus, rotational speed ratio of tool over workpiece and number of cutting tooth also affects the uncut chip area indirectly.
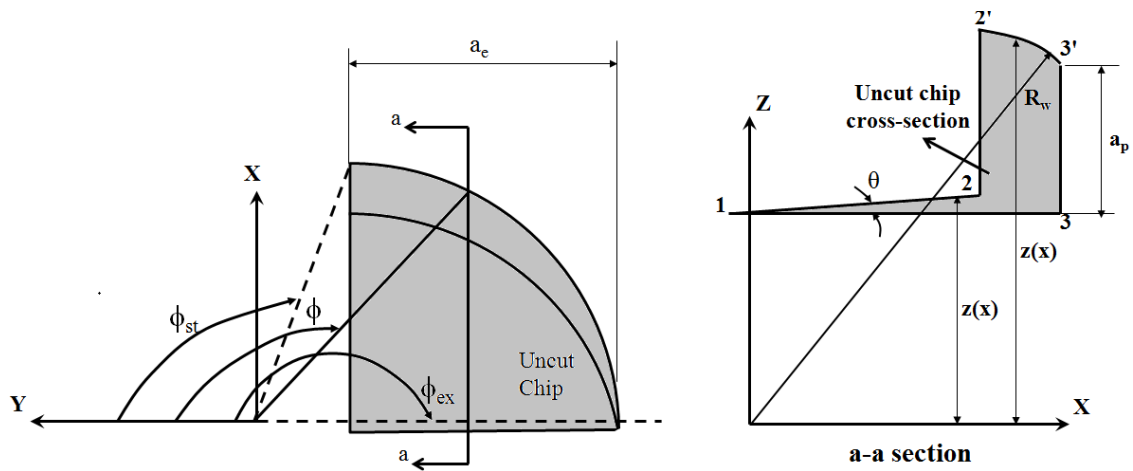
Figure 3-3: Uncut chip cross section in orthogonal turn-milling

Line 1-2 represents the bottom of the tool at previous position and can be formulated by:

$$z(x) = \tan\theta.x + \frac{(R_w - a_p)}{\cos\theta} \tag{3.1}$$

where

$$\theta = \frac{360^\circ}{m * r_n} \tag{3.2}$$

where a_p is axial depth of cut, R_w is radius of workpiece, m is the number of cutting teeth, r_n is the rotational speed ratio of tool over workpiece and x represents the position in the X direction. The line 1-3 is shown in Figure 3-3 as the bottom line of tool at current position can be expressed by;

$$z(x) = (R_w - a_p) \tag{3.3}$$

Arc 2'-3' is on the surface of the workpiece;

$$z(x) = \sqrt{(R_w^2 - x^2)} \tag{3.4}$$

The positions of the points 1, 2 and 3 in X axis, can be formulated by;

$$x_1 = (R_w - a_p) \sin \frac{\theta}{2}$$

$$x_2 = (R_t - ((R_w - a_p) + \tan(\frac{\theta}{2}) \tan \theta) \sin \theta) \cos \theta$$

$$x_3 = R_t \tag{3.5}$$

where R_t is the radius of the cutting tool. At this point one can compute the chip thickness at a desired location since each region has its own governing equation. In the first region which is bounded by lines 1-2 and 1-3, the chip thickness can be found as follows:

$$h(x) = \tan \theta . x + \frac{R_w - a_p}{\cos \theta} - (R_w - a_p) \tag{3.6}$$

The chip thickness in the region, which generated by side edge of the tool, is formed by arc 2'-3' and line 1-3 can be defined as;

$$h(x) = \sqrt{(R_w^2 - x^2)} - (R_w - a_p) \tag{3.7}$$

As can be observed from the Figure 3-3 that feed per workpiece parameter directly effects the start and exit angles. Corresponding start and exit angles can be expressed by;

$$\varphi_{st} = \frac{\pi}{2} + \arcsin \frac{R_t - a_e}{R_t}$$

$$\varphi_{ex} = \pi \tag{3.8}$$

3.1.2. Eccentric Condition

Similar to the centric condition uncut chip formation analogy, cutting tool also removes material with both bottom and side edges. However, the contribution of this tool parts into the total uncut chip area depend on eccentricity parameter. Eccentricity in orthogonal turn-milling changes engagement boundaries and areas, and in turn, the chip

thickness as well. Based on the analysis, uncut chip formation can be separated into three cases due to the effect of eccentricity parameter. For all three cases h represents the chip height in Z direction with respect to x which represents the incremental length along the X axis.
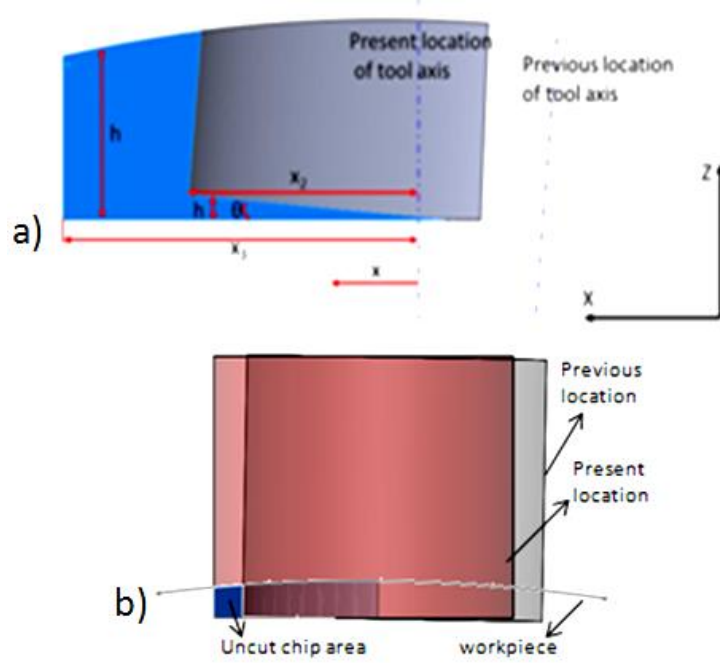
Figure 3-4: Uncut chip cross section for Case 1

Figure 3-4a shows the cross section of uncut chip in Case 1 which represents the configuration where there is a piece of uncut chip beyond the tool axis. Furthermore, Figure 3-4b represents the subsequent tool locations in cutting process which generates the chip. For case 1, the uncut chip thickness can be evaluated by;

If $0<x<x_2$

$$h = \tan(\theta) * x + ((R_w - a_p) * \tan(\theta/2) - e) * \tan(\theta) \tag{3.9}$$

If $x_2<x<x_3$

$$h = \sqrt{R_w^2 - (x-e)^2} - (R_w - a_p) \tag{3.10}$$
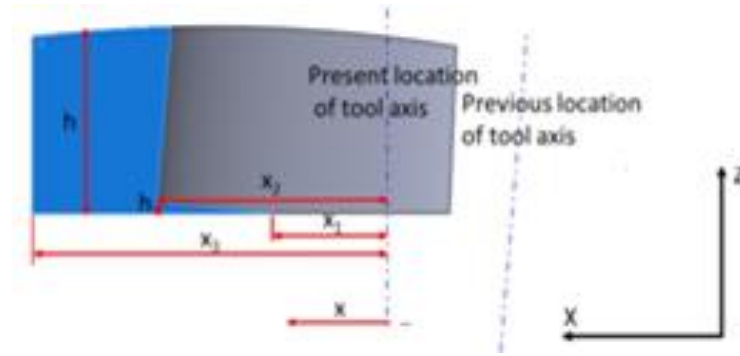
Figure 3-5: Uncut chip cross section for Case 2

Figure 3-5 represents the uncut chip formation in Case 2. When eccentricity is increased, there is no more uncut chip beyond the tool axis and governing equations become as follows;

If $x_1 < x < x_2$

$$h = \tan(\theta) * (x - (e - (R_w - a_p) * \tan(\theta/2))) \tag{3.11}$$

If $x_2 < x < x_3$

$$h = \sqrt{R_w^2 - (x-e)^2} - (R_w - a_p) \tag{3.12}$$
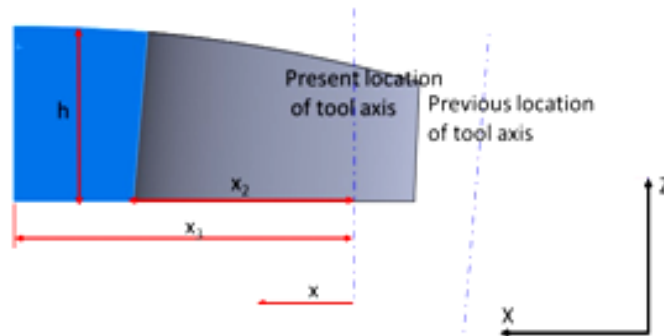
Figure 3-6: Uncut chip cross section for Case 3

After a certain value of eccentricity, chip is formed only by the side edge of the cutting tool.

$$h = \sqrt{R_w^2 - (x-e)^2} - (R_w - a_p) \tag{3.13}$$

When all of these three cases are taken into consideration, uncut chip formation with respect to eccentricity changes can be evaluated. The value of h in Z direction including eccentricity effect is summarized in Table 3-1.

Table 3-1: Chip heights with respect to eccentricity variations

	$0<x<x_2$	$x_2<x<x_3$
Case 1	$h = \tan(\theta) * x + ((R_w - a_p) * \tan(\theta / 2) - e) * \tan(\theta)$	$h = \sqrt{R_w^2 - (x - e)^2} - (R_w - a_p)$
Case 2	$h = \tan(\theta) * (x - (e - (R_w - a_p) * \tan(\theta/2)))$	$h = \sqrt{R_w^2 - (x - e)^2} - (R_w - a_p)$
Case 3	None	$h = \sqrt{R_w^2 - (x - e)^2} - (R_w - a_p)$

Figure 3-7 reflects the uncut chip area in regard to immersion angle for different eccentricity values.
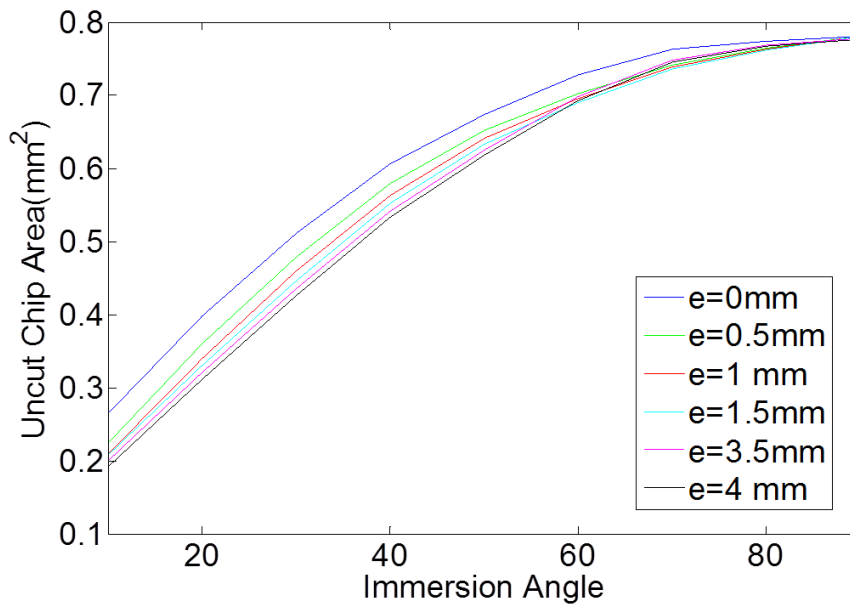
Figure 3-7: Uncut chip area with respect to eccentricity

Used cutting parameters in simulation are; R_t=4mm, a_p=1mm, θ=1° and R_w=45mm. Although Φ_{st} depends on the R_t and a_e, Φ_{ex} is always 180°. The results presented in Figure 3-7 may also be an indication of the fact that the uncut chip area decreases with increasing eccentricity.

3.2. Mechanistic modeling of Turn-milling forces

3.2.1. Identification of cutting force coefficients

Orthogonal cutting coefficients can be generated by performing tube material machining orthogonally in a conventional turning machine. Based on the linear edge force model, orthogonal database can be obtained by taking into consideration different

process parameters by varying uncut chip thicknesses, cutting speeds (V_c) and rake angles (α) etc.
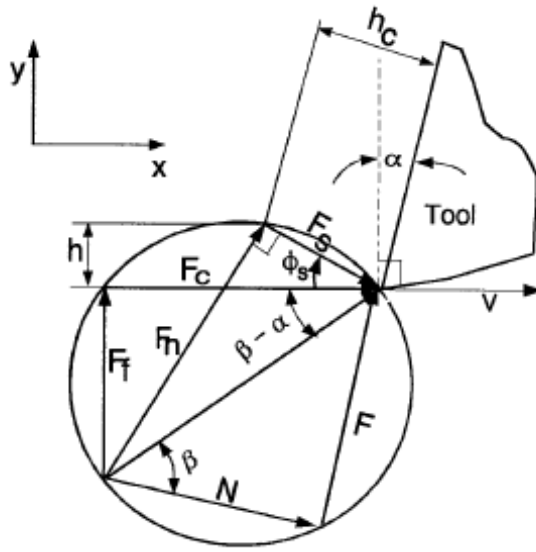
Figure 3-8: Orthogonal cutting force diagram [42]

Obtained milling force coefficients from orthogonal database may not be accurate enough because of the obliquity of cutting tool. For this purpose, coefficients are transformed into oblique cutting conditions by using Armarego's approach [41].

$$K_{tc} = \frac{\tau}{\sin\phi_s} \frac{\cos(\beta_n - \alpha_n) + \tan\eta_c \sin\beta_n \tan\lambda_s}{\sqrt{\cos^2(\phi_s + \beta_n - \alpha_n) + \tan^2\eta_c \sin^2\beta_n}}$$

$$K_{rc} = \frac{\tau}{\sin\phi_s \cos\lambda_s} \frac{\sin(\beta_n - \alpha_n)}{\sqrt{\cos^2(\phi_s + \beta_n - \alpha_n) + \tan^2\eta_c \sin^2\beta_n}}$$

$$K_{ac} = \frac{\tau}{\sin\phi_s} \frac{\cos(\beta_n - \alpha_n)\tan\lambda_s - \tan\eta_c \sin\beta_n}{\sqrt{\cos^2(\phi_s + \beta_n - \alpha_n) + \tan^2\eta_c \sin^2\beta_n}} \text{w} \qquad (3.14)$$
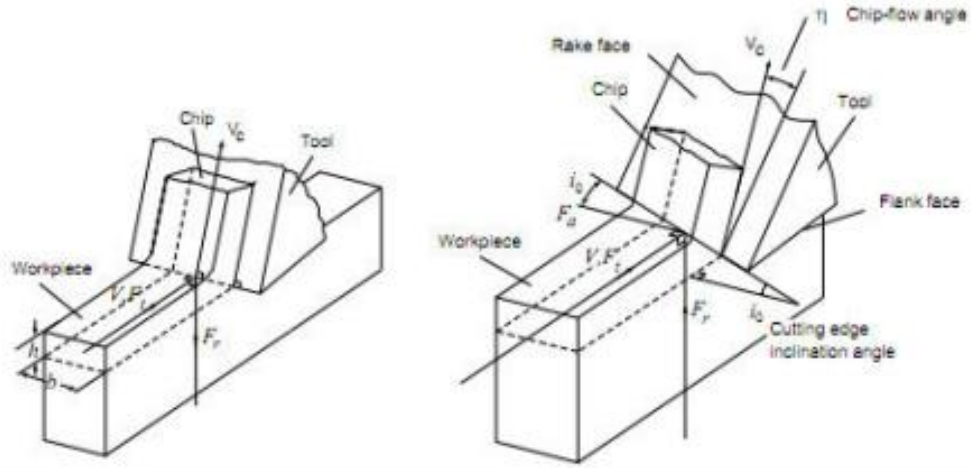
Figure 3-9: Orthogonal and oblique cutting geometries [41]

Shear stress at the shear plane required for cutting force coefficient calculations is formulated by;

$$\tau = \frac{F_c \cos\phi_s - F_f \sin\phi_s}{bh} \sin\phi_s \qquad (3.15)$$

Shear angle is calculated from Merchant's approximation which based on minimum energy principle;

$$\phi_s = \frac{\pi}{2} + \frac{\alpha_n}{2} - \frac{\beta_n}{2} \qquad (3.16)$$

where α_n and β_n represent the normal cutting parameters defined on the oblique shear plane;

$$\alpha_n = \tan^{-1}(\tan\alpha \cos\lambda_s)$$

$$\beta_n = \tan^{-1}(\tan\beta \cos\eta_c) \qquad (3.17)$$

The experimental results indicate that when the chip thickness approaches zero, cutting force converges a value which is different than zero. This situation is the result of sharpness of the tool edge which ends up with ploughing of some material under tool nose and flank contact. Corresponding effect is modeled as edge force by researchers independently [43][44][45]. Due to the physical complexity of modeling the ploughing and flank contact, researchers identified the edge forces experimentally.

3.3. Identification of turn-milling cutting forces

Intermittent cutting characteristics of turn-milling causes periodic forces during operation. Cutting forces of turn-milling are simulated by generating orthogonal to

oblique transformation of cutting data and the chip thickness calculations as discussed in Section 3.1 and 3.2 [35][36]. It should be noted that local chip thickness and instantaneous cutting speed are used in the calculations. After that, within the cutting zone, process forces can be obtained by dividing the uncut chip thickness. The elemental cutting forces can be calculated as follows [42]:

$$dF_{t,j(\phi,z)} = [K_{tc}h_j(\phi j(z)) + K_{te}]dz$$

$$dF_{r,j(\phi,z)} = [K_{rc}h_j(\phi j(z)) + K_{re}]dz$$

$$dF_{a,j(\phi,z)} = [K_{ac}h_j(\phi j(z)) + K_{ae}]dz \tag{3.18}$$

K_{tc}, K_{rc} and K_{ac} are the cutting force coefficients and they are evaluated by oblique transformation to orthogonal cutting data. K_{te}, K_{re} and K_{ae} are the edge force coefficients which are identified by linear edge force model. The elemental cutting forces are integrated within engagement boundaries to calculate the total process forces as follows:

$$F_t(\phi_j(z)) = \int_{z_{j,1}}^{z_{j,2}} dF_t(\phi_j(z))dz$$

$$F_r(\phi_j(z)) = \int_{z_{j,1}}^{z_{j,2}} dF_r(\phi_j(z))dz$$

$$F_a(\phi_j(z)) = \int_{z_{j,1}}^{z_{j,2}} dF_a(\phi_j(z))dz \tag{3.19}$$

where $z_{j,1}(\phi_j(z))$ and $z_{j,2}(\phi_j(z))$ are the engagement limits of the in-cut portion of tooth j.

a)   **b)**

Figure 3-10: a) Mori Seiki NTX 2000 machine tool b) Experimental setup for cutting force measurements

In addition to the experimental apparatus which are illustrated in Figure 3-10, Kistler Multichannel signal conditioner (Type 5223) was used. In addition, 10 mm diameter

solid carbide end mill with 4 teeth and AISI 1050 steel workpiece were selected. Test equipments and used material were described in Section 2 in detail.

3.4. Simulation and experimental results

As discussed earlier, verification tests of cutting force model were performed on Mori Seiki NTX2000 multi-axis machine tool. The comparison of simulated and calculated resultant force results for AISI 1050 steel can be seen in Figure 3-11 where cutting parameters were selected as follows; n_t=2000 rpm, n_w=20 rpm, a_p=0.5, e=0 mm and a_e=0.3 mm/rev. Cutting force coefficients are calculated by using Eq. 3.14. After that, by performing oblique transformation of orthogonal cutting data, K_{tc}=1537 N/mm², K_{rc}=507 N/mm² and K_{ac}=460 N/mm² are found. Additionally, edge force coefficients are obtained from experimental calibrations tests as K_{te}=150 N/mm, K_{re}=150 N/mm and K_{ae}=0. Compared to the conventional milling operation, it can be deduced that edge force coefficients for turn-milling are relatively high because of the engagement limits of tool and workpiece.
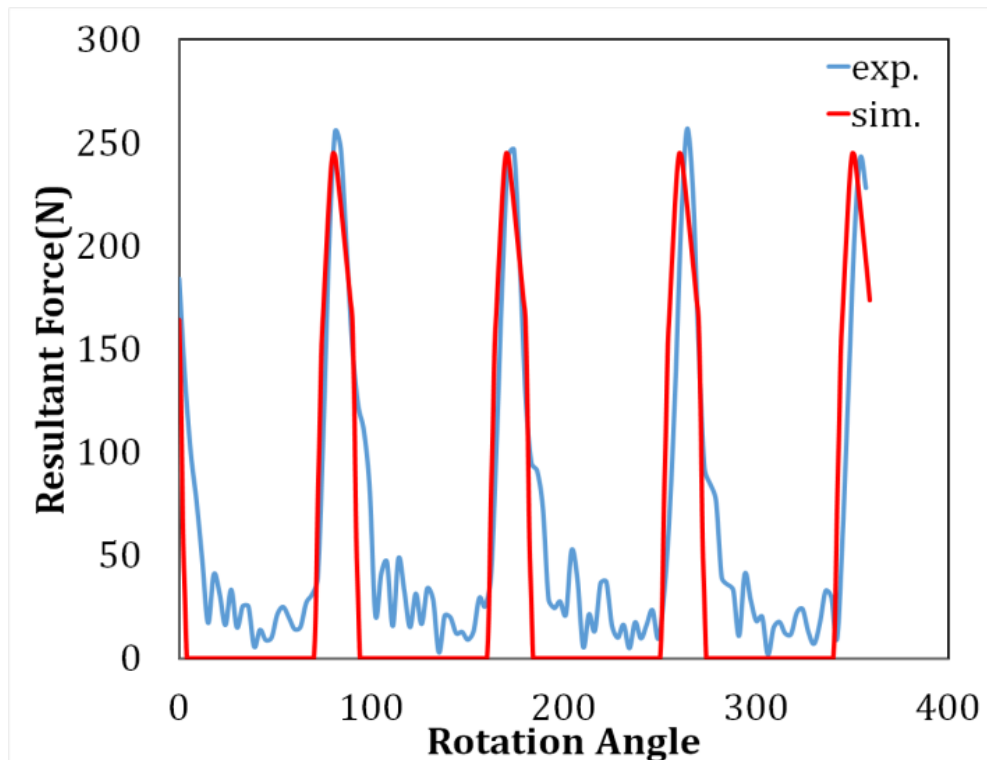
Figure 3-11: Measured and simulated resulted force results for turn-milling

As it can be seen in Figure 3-11, maximum resultant cutting force is obtained as 250N. Moreover, a good agreement is found between the model predictions and experimental

data. Fluctuated results between periodic peaks of experimental data are obtained due to the noise during measurement.

Another cutting test simulation was conducted by using different values of r_n , a_p and a_e in order to find out the effects of cutting parameters and the results are shown in Figure 3-12. The selected cutting conditions for measured and simulated cutting forces are summarized in Table 3-2. The simulations are done by using the proposed models.

Table 3-2: Cutting parameters used in turn-milling tests

Test No	R_w (mm)	R_t (mm)	n_t (rev/min)	n_w (rev/min)	r_n	a_p (mm)	a_e (mm)
1	45	5	3000	20	150	0.5	0.3
2	45	5	2000	20	100	0.5	0.3
3	45	5	2000	20	100	0.5	0.6
4	45	5	2000	20	100	1	0.6
5	45	5	4000	20	200	1	0.6
6	45	5	4000	20	200	1	0.3

Observing the results given in Figure 3-12, it can be clearly deduced that the predictions are very close to the experimental measurements. In general terms, cutting forces increase with increasing a_e and a_p, and decrease with increasing r_n ratio.
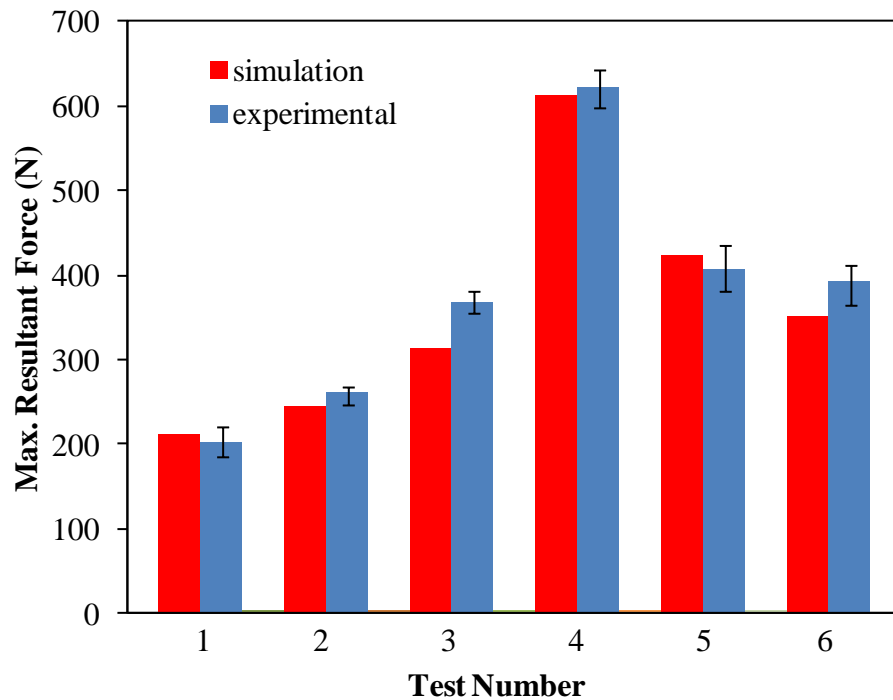
Figure 3-12: Maximum resultant forces with respect to different cutting conditions

By changing n_t and n_w with the same rate, r_n remains constant but cutting speed changes because of n_t variation. In essence, constant ratio may also change the cutting forces due to its indirect effects on cutting force coefficients. In other words, cutting speed affects cutting temperature and strain rate within the deformation zone as well as friction condition on rake contact. Thus, based on the thermal stability of the workpiece material, forces may increase or decrease with respect to cutting speed. Additionally, according to the study represented Astakhov's study [47], increase in cutting speed causes cutting temperature and contributes to reduce tool life. The maximum and average differences between the proposed model predictions and the experimental results are 12% and 5%, respectively which is mainly due to the inaccuracy in the material model and from measurement errors.
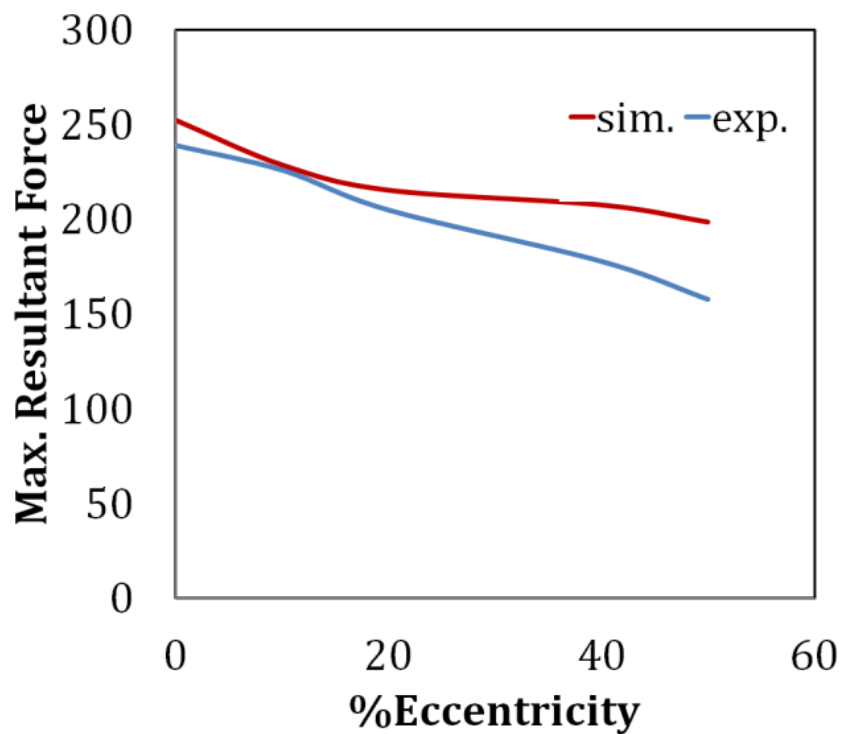
Figure 3-13: Maximum resultant cutting forces with respect to eccentricity variations

Used cutting parameters for effect of eccentricity on cutting force test are summarized as follows; a_p=0.5mm, a_e=0.5mm/rev and r_n =250. Moreover, eccentricity is selected %0, 10, 20, 40 and 50 of tool diameter and the results of both simulation and calculation are illustrated in Figure 3-13. It can be obviously deduced from the figure that maximum resultant cutting forces diminish with increasing eccentricity. Based on the results illustrated in Figure 3-7, increasing eccentricity reduces the uncut chip area and that causes the decrease in cutting force as it is expected. With raising eccentricity, the area under bottom part of the cutting tool reduces. Additionally, beyond a certain value

of eccentricity, only side edges f cutting tool contribute to generation of chip formation. The maximum and average discrepancies are 19% and 7%, respectively which is mainly due to the effect of eccentricity on edge force coefficients. One can interpret form the figure that edge forces are also change with respect to eccentricity parameter. During the simulation fixed edge force coefficients are used, thus the difference between calculated and simulated data comes from this approach.

3.5. Summary

In this section, chip formation mechanism with respect to eccentricity variation is analytically modeled at first. Since, uncut chip geometry and engagement limits are crucial from cutting force, cutting temperature and stability points of views. After instantaneous chip area calculation, which is also necessary for interpretation of eccentricity effect on tool life, required process parameters in order to implement semi-analytical force model approach are identified. Corresponding data are obtained from orthogonal cutting tests and then used in orthogonal to oblique transformation procedure. A good agreement is observed between the simulated and calculated cutting force results. For centric orthogonal turn-milling case, the maximum and average discrepancies are 12% and 5%, respectively. On the other hand, for the eccentric turn-milling case, the maximum difference between the proposed model predictions and the experimental results are around 19% whereas the average error is around 7%.

CHAPTER 4

4. MATERIAL REMOVAL RATE AND SURFACE QUALITY

Increasing the productivity of available facilities is considered to be one of the most important factors for manufacturing industry. However, the necessary quality requirements need to be fulfilled simultaneously. Manufacturing time, cost and surface quality which are key elements of productivity, are affected by process parameter selection from different scenarios. With the development on higher strength materials, which retain their mechanical properties even at elevated temperatures, there has been an increased demand on researches to define proper machining methods for them. In order to cope with such variety of engineering scenarios, multi-axis machining operations were designed. Turn-milling process, which designed to be a remedy for such kind of machining requirements, has to be modeled.

In this section, analytical models for surface generation and selection of process parameters for increased productivity in orthogonal turn-milling operations are presented.

4.1. Material Removal Rate

MRR is an indicator of the productivity and represents as removed material volume in unit time. MRR is proportional to the axial and radial depth of cuts similar to the conventional milling process as expressed in Eq. 4.1. Actually a_e in this equation has the same role of radial depth of cut in conventional milling, and should be used in the same way in MRR calculation. MRR can be calculated as follows:

$$MRR = v_f * a_p * a_e$$

$$v_f = m * n_t * f_z$$

$$f_z = \frac{2 * \prod * R_w * n_w}{n_t * m}$$

(4.1)

where a_e is the feed per workpiece revolution, a_p is axial depth of cut, v_f is the feed speed, m is the number of cutting edges, f_z is feed per tooth, n_t is rotational speed of the tool and n_w represents the rotational speed of the workpiece. For the constant n_t, if R_t increases, cutting speed also increases. Moreover, as it can be understood from the formula of f_z that R_w has a direct proportion with f_z.
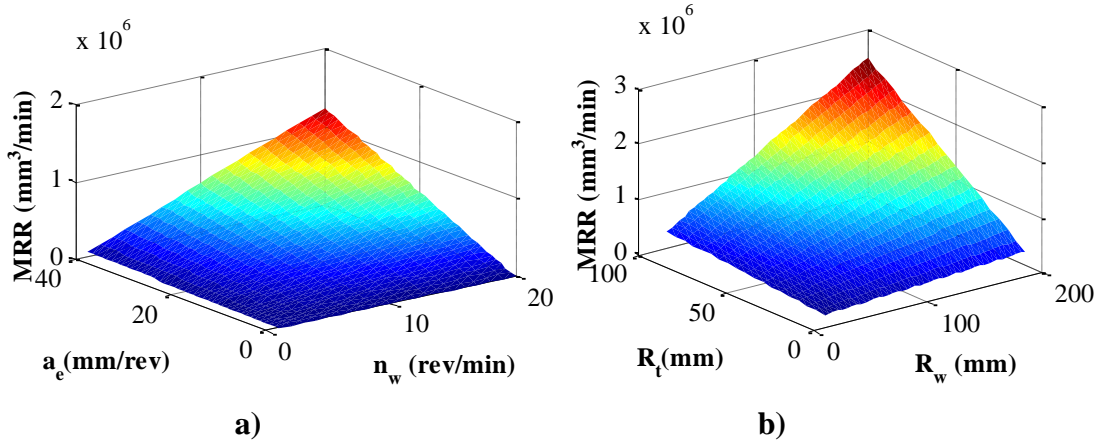
Figure 4-1: Effects of n_w, a_e, R_t and R_w on MRR

Defined cutting parameters in simulation are as follows; a_p=5 mm, e=21 mm, m=2. It can be understood from Figure 4-1a that MRR increases by increasing a_e and n_w. In the event of f_z is kept constant, n_t has no effect on MRR, so n_w is selected as a parameter instead of r_n as shown in Figure 4-1a. Additionally, another important outcome is that increasing R_t and R_w results in increasing MRR as illustrated in Figure 4-1b.

4.2. Form Errors

Although turn-milling process potentially can generate high MRR, it has some drawbacks and limitations. Form errors, which result of high MRR in turn-milling, are represented in Figure 4-2.
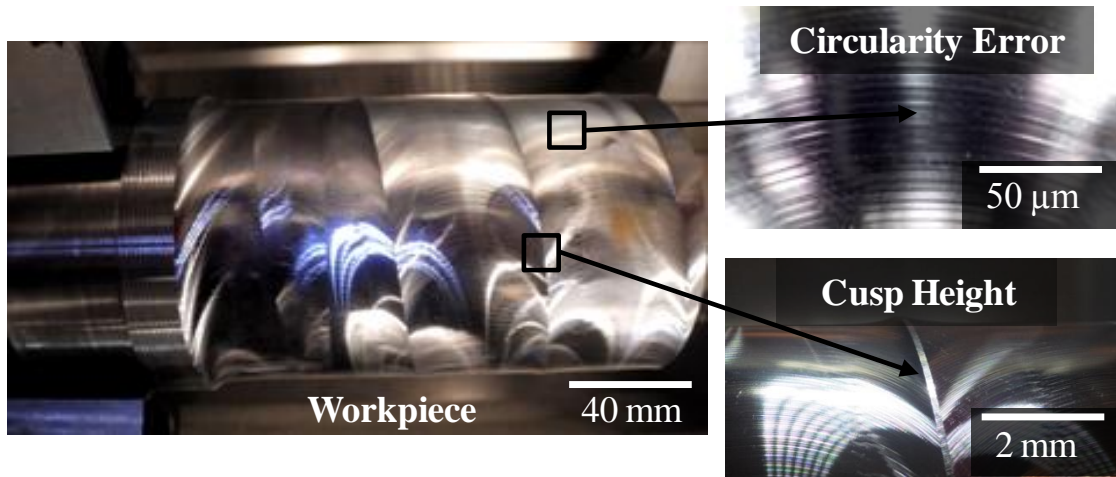
Figure 4-2: Form errors in turn-milling where circularity error (OB-OA) is 0.3µm and cusp height (ch) is 0.5mm

4.2.1. Circularity

Turn-milling produces non–cylindrical surfaces due to the combined rotations of workpiece and tool. Circularity error, which is shown in Figure 4-2, is a result of interrupted cutting and simultaneous rotation of milling tool and workpiece, so that the final cross section of machined part in turn-milling is a polygon.
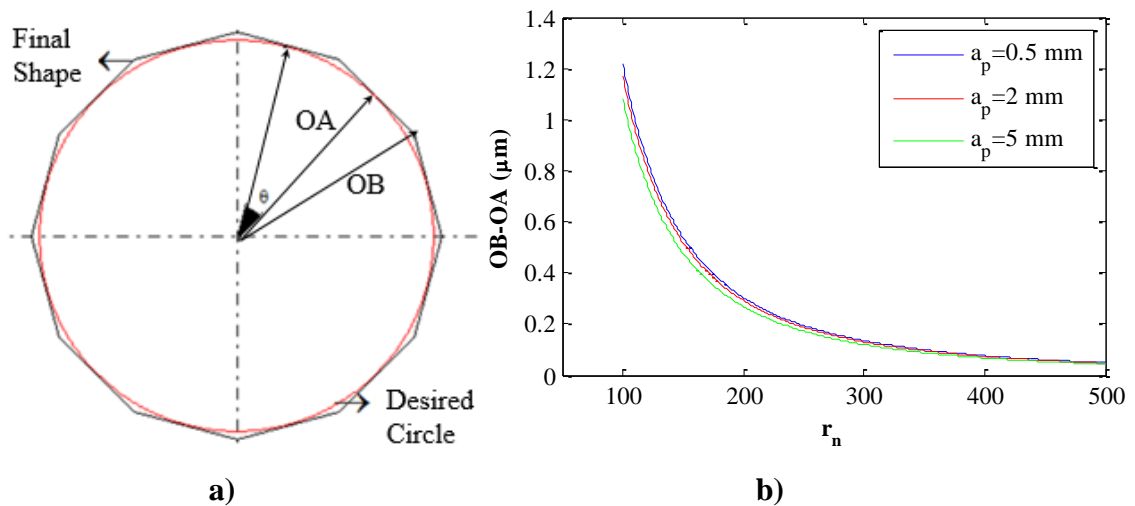
Figure 4-3: a) Circularity error b) Circularity error with respect to a_p and r_n

As it can be seen from Figure 4-3a that obtained form is a polygon. The difference between the desired circle and final shape is denoted by *OB-OA* is the circularity error and can be formulated as follows:

$$OA = R_w - a_p$$

$$OB = \frac{R_w - a_p}{\cos \theta}$$

$$OB - OA = (R_w - a_p) * (\frac{1}{\cos \frac{\theta}{2}} - 1) \qquad (4.2)$$

In orthogonal turn-milling, as the cutting edge engages with the work while it rotates, the work surface also moves due to the simultaneous workpiece rotation. It results in a certain time period where there is no contact between the cutting edge and the finished surface until the next tooth reaches to the finished surface. The time period between these two contact instants of the subsequent teeth with the finished surface determines the facet width. Thus the number of facets on the periphery of the cylindrical workpiece. The time between subsequent cutting tool engagements with workpiece is the main parameter which directly affects the number of facets on the machined surface. Eq. 4.3 illustrates the geometrical implementation of θ angle, which represents the angle between subsequent facet middle points and related to number of facets. It can be calculated as:

$$r_n = n_t / n_w$$

$$\theta = \frac{360^{\circ}}{z \, x \, r_n} \qquad (4.3)$$

where n_t is the rotational speed of tool, n_w is the rotational speed of the workpiece and r_n represents the rotational speed ratio of tool over workpiece.

A final observation from the equation above is that, eccentricity has no effect on number of facets (circularity form error). On the other hand, the effect of a_p and r_n on circularity form error can be seen in Figure 4-3b. Although a_p has a slight effect on circularity, r_n effects this form error substantially. Supporting this observation, in order to reduce the circularity form error, r_n should be increased.

4.2.2. Cusp Height

Cusp which is another circumferential form error in turn-milling shown in Figure 4-2 is the height of the remaining material on the surface due to the tool motion and is directly associated with the tool and workpiece diameter as well as step over. Step over can be

43

defined as the part of the cutter's diameter engaged in a cut. In conventional milling processes feed rate and cutting tool radius have direct effects on the cusp height. a_e in turn-milling process is equivalent to radial depth of cut in conventional milling process. Therefore, increasing a_e in order to achieve higher MRR, results in high cusp height.
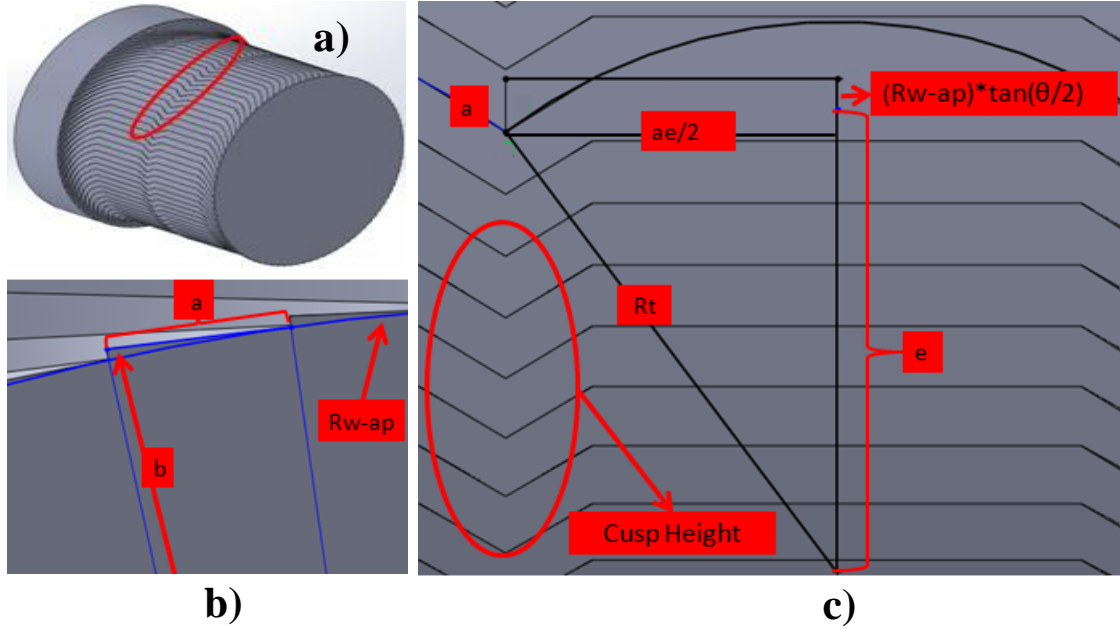
Figure 4-4: a) Isometric view, b) side view and c) top view of turn-milled part

Figure 4-4a shows the cusp height formation on a turn-milled part. Figure 4-4b and Figure 4-4c represent the methodology of analytical cusp height formulation. As shown in Figure 4-4c;

$$a = \left(\left[e + \left[(R_w - a_p) * \tan\left(\frac{180^\circ}{z * r_n} \right) \right] \right] - \left[\sqrt{(R_t)^2 - \left(\frac{a_e}{2} \right)^2} \right] \right) \tag{4.4}$$

From Figure 4-4b;

$$b = \sqrt{(R_w - a_p)^2 + (a)^2} \tag{4.5}$$

Cusp height is derived by substituting Eq. 4.4 into Eq. 4.5;

$$ch = \sqrt{(R_w - a_p)^2 + \left(\left[e + \left[(R_w - a_p) * \tan\left(\frac{180^\circ}{z * r_n} \right) \right] \right] - \left[\sqrt{(R_t)^2 - \left(\frac{a_e}{2} \right)^2} \right] \right)^2} - (R_w - a_p) \tag{4.6}$$

where ch is cusp height, R_w radius of workpiece, e is eccentricity, m is number of cutting tool teeth and R_t is radius of cutting tool. When a is equal to zero which means there is

no cusp and given in Eq. 4.4, critical feed per workpiece revolution value (a_{ecrit}) is obtained as;

$$a_{ecrit} = 2 * \sqrt{(R_t)^2 - \left(e + \left[(R_w - a_p) * \tan\left(\frac{180°}{z * r_n} \right) \right] \right)^2} \qquad (4.7)$$

a_e can be increased up to the critical value, which is represented by the equation above, without producing any cusp. By this way, MRR can be increased without sacrificing surface quality. a_{ecrit} represents the projected length (P_L) of tool onto workpiece as shown in Figure 3-1. If a_e is higher than this value, tool leaves behind uncut surface which is cusp height of the workpiece.

Effects of a_e, r_n, R_w and R_t on cusp height based on simulations used by Eq. 4.6 are illustrated in Figure 4-5.
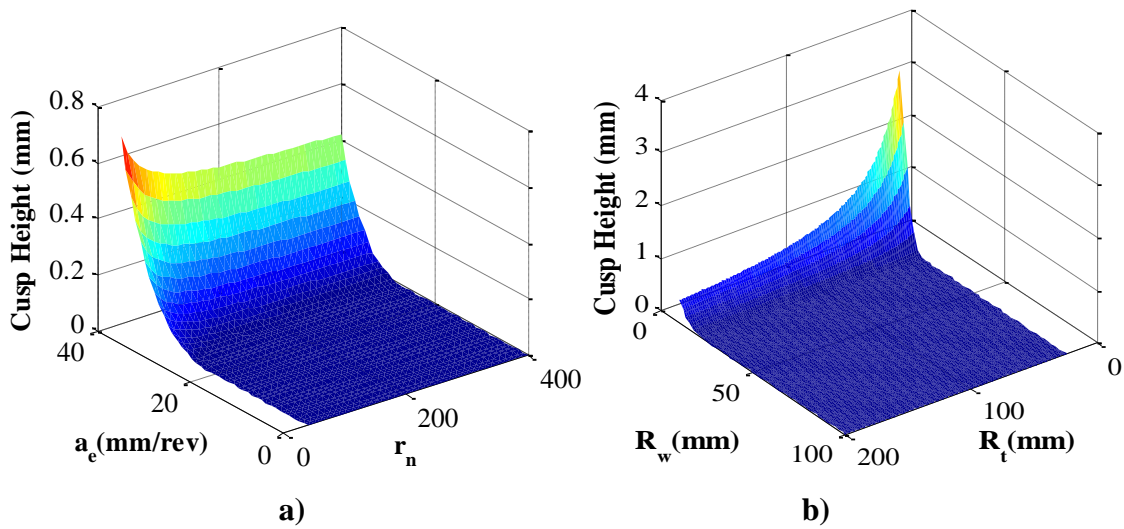
Figure 4-5: Variations of cusp height with respect to process parameters

Selected cutting parameters in simulation are; a_p=5mm, e=21mm (optimum eccentricity value for this tool-workpiece configuration), m=4, n_t=2000rpm, n_w=10rpm, R_t=25mm and R_w=50mm. It can be deduced from the Figure 4-5a that cusp height decreases by increasing r_n. In order to increase r_n, n_t can be raised which also contributes to increase MRR. On the other hand, n_t is restricted by suggested cutting speed from the point of tool life. As an example, cutting tool manufacturer's suggest that selected cutting speed for difficult-to-cut materials machining such as Waspaloy, Inconel 718 and Ti6Al4V must be equal or lower than 40m/min. Moreover, n_w can be diminished for increasing r_n. Based on Figure 4-5b, tool radius has more impact than workpiece radius on cusp height. Moreover, n_t can be limited by the maximum tool spindle speed of the machine

tool. Due to power limit of the machine tool, this problem could be confronted in turn-milling operations which are performed with live tooling system on conventional turning center.
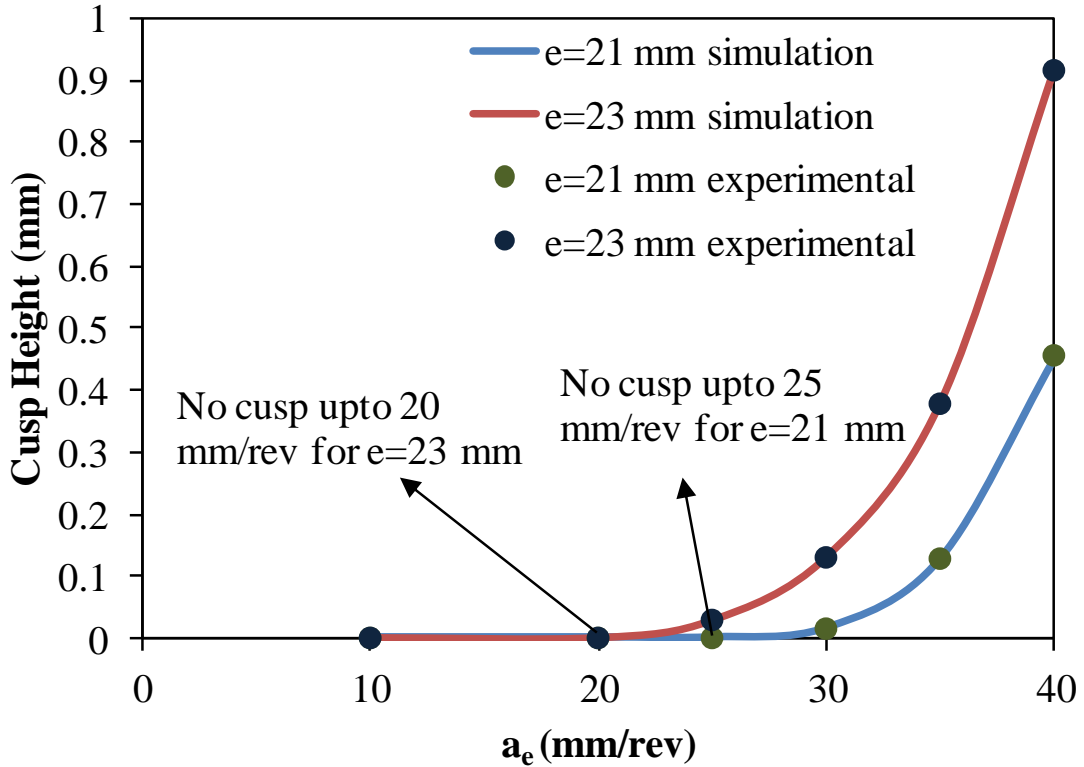
Figure 4-6: Verification of the cusp height model with respect to a_e and e parameters

Figure 4-6 illustrates both analytical and experimental results for the cusp height. As can be seen, a very good agreement is found between the model predictions and the experimental data. A final observation from the data presented is that up to a certain a_e value there is no cusp regardless of the eccentricity. However, when a_e is defined over that defined value (Eq. 4.7), cusp height increases dramatically. For instance, when e=23mm a_e can be increased up to 20mm/rev otherwise there will be cusp on machined surface. On the other hand, when e=21mm which is optimum eccentricity value for used cutting tool, a_e can be defined as 25mm/rev without facing any cusp on machined surface. For two cases investigated in the graph above, by using optimum eccentricity, a_e can be increased by25% without sacrificing any surface quality. This is an important outcome in terms of productivity in turn-milling.

4.2.3. Circumferential Surface Roughness

Cutting tool follows a helical path as shown in Figure 4-7a due to the simultaneous rotational movements of tool and workpiece. As shown in Figure 4-7a, higher a_e results in feed marks which have higher helix angles on the surface.
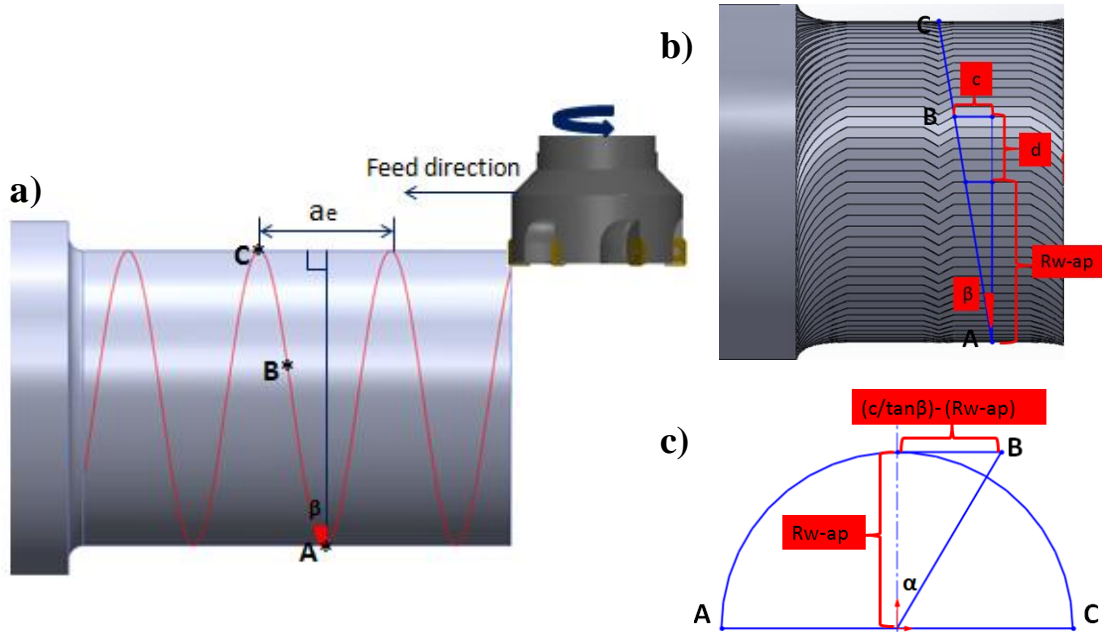
Figure 4-7: a) Workpiece 3D, b) projected length and c) angle α representation

The angle between this trochoidal path and the normal line is given by Eq. 4.8 which is derived from the triangle between sequential tool path revolutions.

$$\beta_f = \arctan\left(\frac{a_e}{4*(R_w - a_p)}\right) \tag{4.8}$$

Feed mark angle (β_f) affects the circumferential roughness indirectly. As can be observed from the Figure 4-7b, corresponding angle changes the slope of the feed marks on workpiece. In circumferential surface roughness measurements, the probe or needle contacts with the workpiece at number of points are at the same height from a base plane and equally located around the workpiece. As a result of this, the probe touches circular form errors and cusps because of the feed mark angle on the workpiece.

As illustrated in Figure 4-7b, c represents half of the projected length ($P_L/2$);

$$c = \sqrt{(R_t)^2 - \left(e + \left[(R_w - a_p)*\tan\left(\frac{180^\circ}{z*r_n}\right)\right]\right)^2} \tag{4.9}$$

and angle α is calculated as from the triangle represented in Figure 4-7c;

$$\alpha = \arctan\left(\frac{\dfrac{\sqrt{(R_t)^2 - \left(e + \left[(R_w - a_p) * \tan\left(\dfrac{180^{\circ}}{z * r_n}\right)\right]\right)^2}}{\tan\beta_f} - (R_w - a_p)}{(R_w - a_p)}\right) \tag{4.10}$$

Circumferential surface roughness contains both cusp and circularity form errors. In order to formulate the circumferential surface roughness, workpiece surface is divided into two parts which are determined by A, B and C points as shown in Figure 4-7. Point B represents the starting point of cusp height effect. Until point B, only circularity is observed on the workpiece. Between point B and C, cusp effect involves in surface roughness calculations and increases linearly. The circumferential roughness is obtained from the following relation:

$$circ_{rough} = \left(\frac{90^{\circ} + \alpha}{180^{\circ}}\right) * \left[\frac{(R_w - a_p)}{\cos(\theta/2)} - (R_w - a_p)\right] + \left(\frac{90^{\circ} - \alpha}{180^{\circ}}\right) * \frac{ch}{2} \tag{4.11}$$

Because of rotational symmetry of workpiece, only half of the workpiece was taken into consideration. After point B, cusp height takes place in circumferential surface roughness and increases linearly until point C where it takes its maximum value. On the other hand, constant circularity is observed on machined surface through the path. Moreover, if a_e is selected lower than a_{ecrit}, there will not form any cusp height. At this case, circumferential surface roughness will consist of only circularity form error.
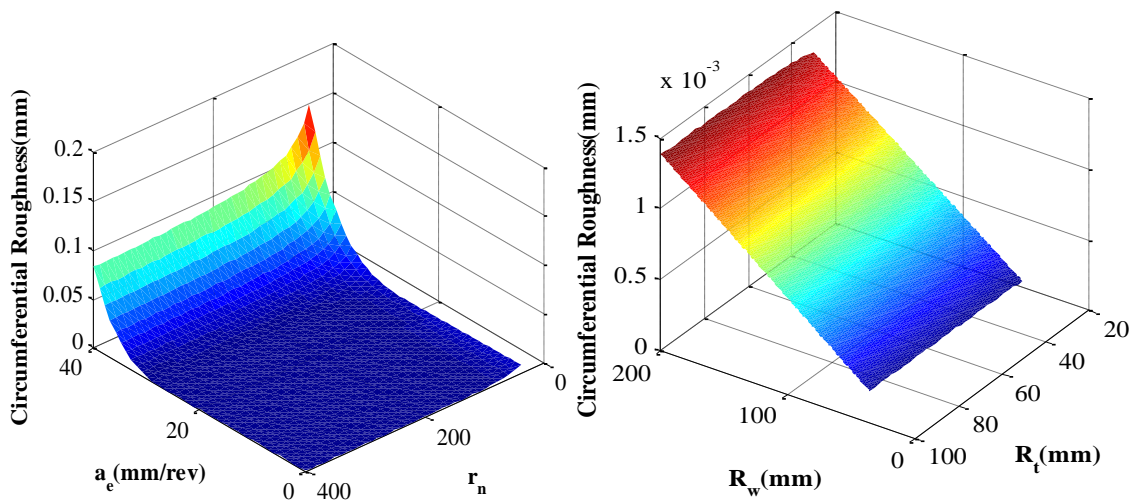
Figure 4-8: Simulations for circumferential surface roughness

Figure 4-8 shows the simulations are done by proposed model. According to Figure 4-8a, increasing r_n and reducing a_e result in decreasing circumferential surface roughness. On the other hand, conversely to the cusp height simulations, workpiece radius has bigger impact on surface roughness than tool radius as illustrated in Figure 4-8b.

4.3. Wiper insert effect on surface roughness

Because of the simultaneous rotations of tool and workpiece in turn-milling operations, surface roughness is affected by a relatively high number of factors at this process. In conventional processes, surface roughness generally depends on the feed rate and size of an insert's nose radius parameters. Traditionally it is understood that surface roughness increases with increased feed rate and decreases with larger tool nose radius.
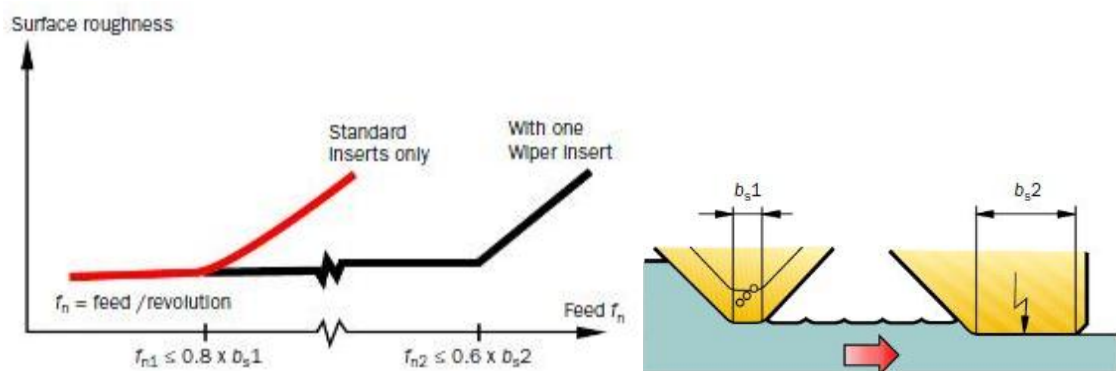
Figure 4-9: Wiper inserts [9]

The wiper inserts, which have modified radial corner to clean the surface, remove more material with their back side. In other words, this kind of inserts increase the tool workpiece engagement length. On the other hand, increasing compressive forces is the main drawback of using wiper insert in machining operation. Figure 4-9 is taken from Sandvik Coromat catalogue, which is one of the well-known cutting tool manufacturers,

and illustrates the wiper insert geometry. b_s1 and b_s2 represents standard and wiper insert parallel land lengths respectively.

Similar to the conventional milling operations, using wiper insert can reduce the surface roughness alongside direction in turn-milling operations. In order to determine the effect of insert type on surface roughness, certain tests were conducted for both standard and wiper inserts with respect to different eccentricity values as shown in Figure 4-10.
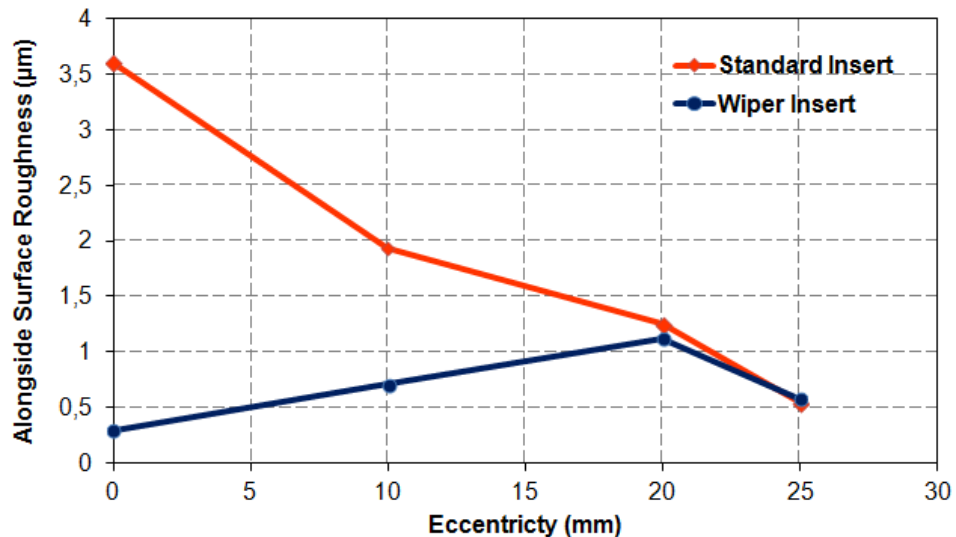
Figure 4-10: Comparison of wiper and standard insert effect on surface roughness

Cutting parameters used in the experiments can be summarized as follows: a_e =3mm/rev m=4, n_t =2000rpm, n_w =20rpm. For wiper insert tests, only one insert of the cutting tool was selected as wiper other three insert were standard. Position of wiper insert in z axis has to be adjusted approximately by 2% upper than standard inserts to prevent tool breakage. Additionally, it should be noted that number of wiper insert in a cutting operation has to be determined according to the feed per tooth value. If feed per tooth value is higher than the parallel land length of the wiper insert, cutting tool will leave behind uncut surface. Thus, in order to prevent this undesirable situation, number of wiper inserts has to be increased. However, there are some drawbacks of using excessive amount of wiper insert in machining operations. Due to the parallel land length of wiper insert's, ploughing effect of cutting tool increases substantially, so cutting force is increased. In essence, number of wiper inserts has to be determined carefully.

Based on the observations obtained from Figure 4-10, for standard insert test condition, when eccentricity is increased, surface roughness decreases drastically. On the other

hand, surface roughness increases with increasing eccentricity until a certain value for wiper insert test condition. Between optimum and maximum eccentricity values, raising eccentricity decreases the chip width as illustrated in Figure 4-11.
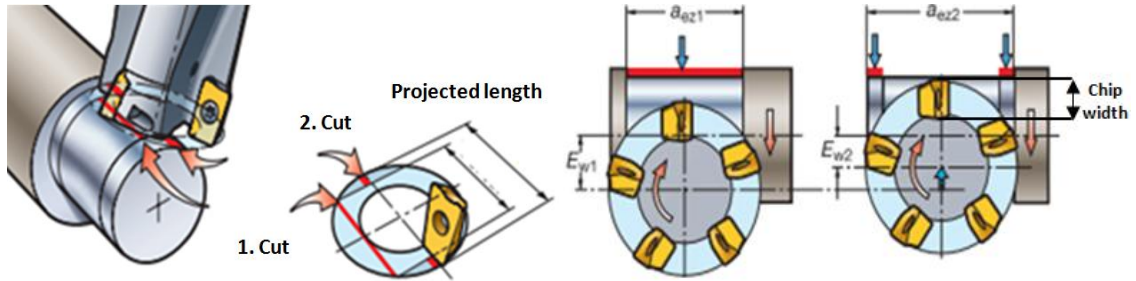
Figure 4-11: Eccentricity effect on projected length [9]

Moreover, when eccentricity becomes equal to the cutter radius only side edges of the cutting tool participate in cutting process. A final observation from the experiment is that there is no worthwhile relationship between r_n and surface roughness. As a result, r_n can be increased as much as possible.

Machine surface produced by the wiper insert is always better than with the ones generated by standard inserts for corresponding feed rate. Based on this conclusion, for the same acceptable surface roughness limit, feed rate for wiper insert case can be defined higher than standard insert case one. Hereby, productivity can be increased without diminishing surface quality. Using the same cutting conditions, for some cases up to 10 times better surface roughness was achieved with wiper insert in orthogonal turn-milling.

4.4. Parameter decision making for MRR

Market demands for higher quality, reduced leads times and cost often create need for alternative manufacturing processes. Within this context, turn-milling, may offer advantages as a promising technology. If the conditions and parameters are selected properly, this relatively new process may provide high productivity and surface quality at the same time especially for different-to-machine materials. For this purpose, surface form errors were analytically modeled and verified at previous sections. In this section, the interaction between these parameters will be investigated. The cutting parameters selected for the following simulations can be summarized as; a_p=5mm, R_w=50mm, m=4, R_t=25mm and r_n=200.
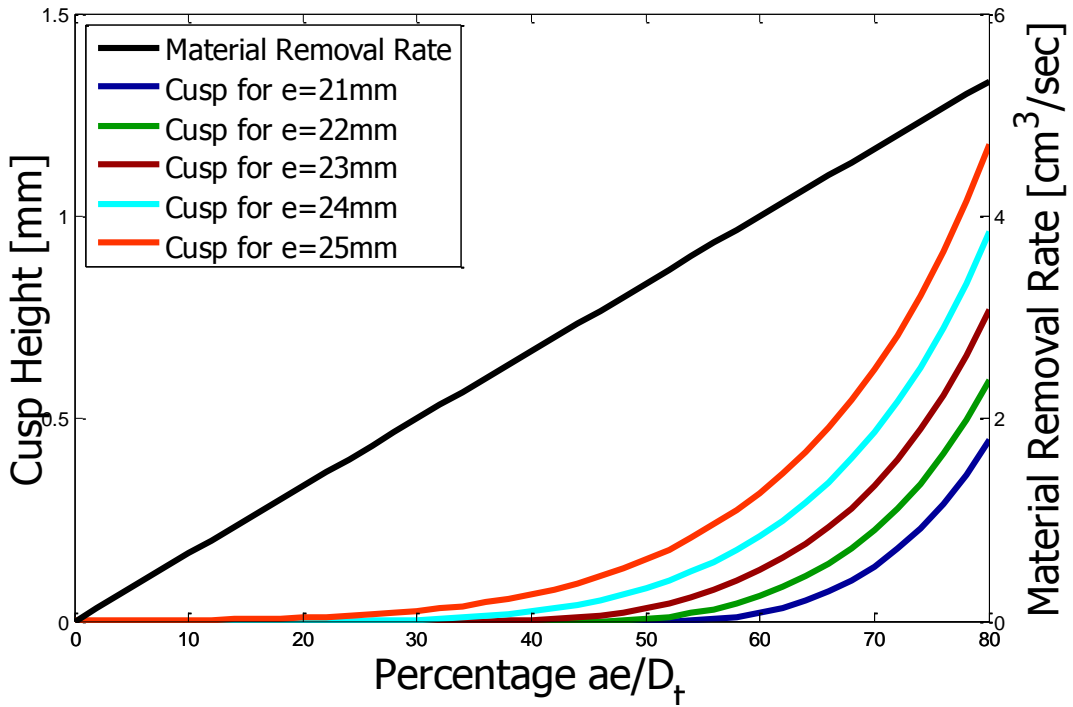
Figure 4-12: Investigation of a_e effect on turn-mill parameters

Figure 4-12 point outs eccentricity and feed per workpiece revolution percentage with respect to tool diameter effects on cusp height. Based on the figure, for the same a_e value, cusp height increases with respect to increasing eccentricity. Additionally, an increase in the amount of the a_e results in higher MRR which represents the productivity.
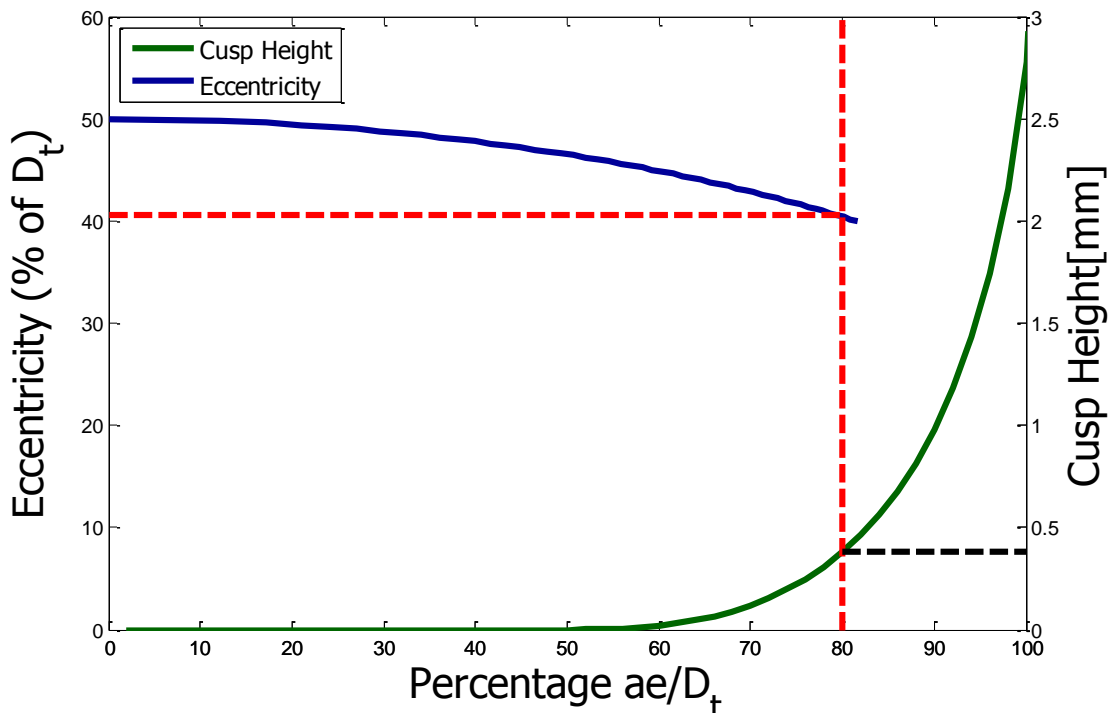
Figure 4-13: Parameter selection criteria

Although increasing MRR decreases the manufacturing time, it also increases the cusp height. Because of the a_e effect on both cusp height and MRR, this parameter has to be selected carefully. Within this context, first a_e parameter has to be selected based on an acceptable cusp height value. Then, eccentricity parameter, which corresponds to selected a_e parameter, has to be set. Figure 4-13 represents this procedure in detail. When percentage a_e/D_t value is raised from 60% to 80%, both cusp height and MRR are increased by 86% and 25% respectively.

4.5. Summary

In this section, clear advantages are identified for orthogonal turn-milling operations including high material removal and deposition rates, geometrical precision and surface integrity. Based on the proposed models, one of the important outcomes is that by defining optimum eccentricity a_e can be increased up to defined value without reducing surface quality. As a result, thanks to the eccentricity parameter, productivity can be increased drastically for the same surface quality. Analytical models for effective process parameter selection in terms of productivity and form errors are introduced. Due to the multi-axis movement of turn-milling process, there is variety of process parameters for this machining process. In order to fulfill the requirements and perform the process effectively, parameters must be selected properly. For that reason, a parameter selection criterion is introduced.

CHAPTER 5

5. TOOL WEAR

In turn-milling process, chip is generated similar to the conventional milling process. Depends on the radial depth of cut value, cutting tooth cools down during a particular amount of time within each tool rotation. The ventilation effect of the tool obtains to maintain lower cutting temperatures and allows decreased workpiece deformations. As a result, generated heat is dissipated around cutting tool and heating of the same section of tool is prevented. For the same cutting conditions, intermitted cutting produces less cutting temperature than in continuous rivals [26]. Figure 5-1 shows the intermitted characteristics of turn-milling.
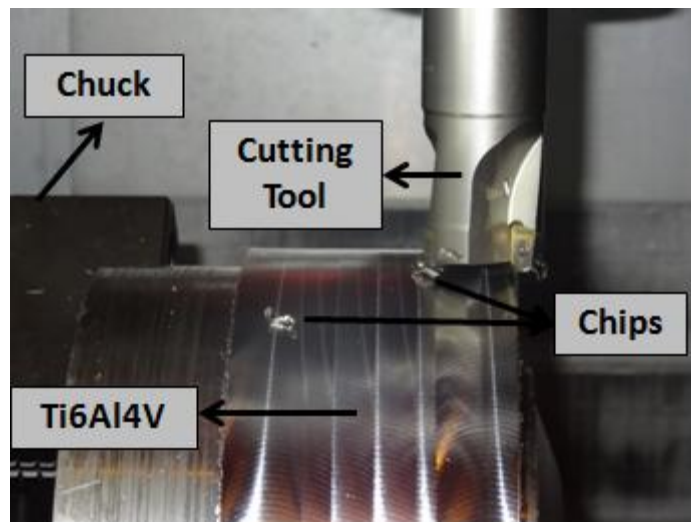
Figure 5-1: Representation of intermitted characteristics of turn-milling

In this section, advantages of turn-milling operations in terms of tool life and the effect of eccentricity and tilt angle on tool life are presented.

5.1. Experimental procedure

Tool wear tests were implemented on Mori Seiki NTX2000 machine tool under three different cooling conditions with constant cutting speed while the flank wear on the inserts was measured periodically by using Nano Focus μSurf.
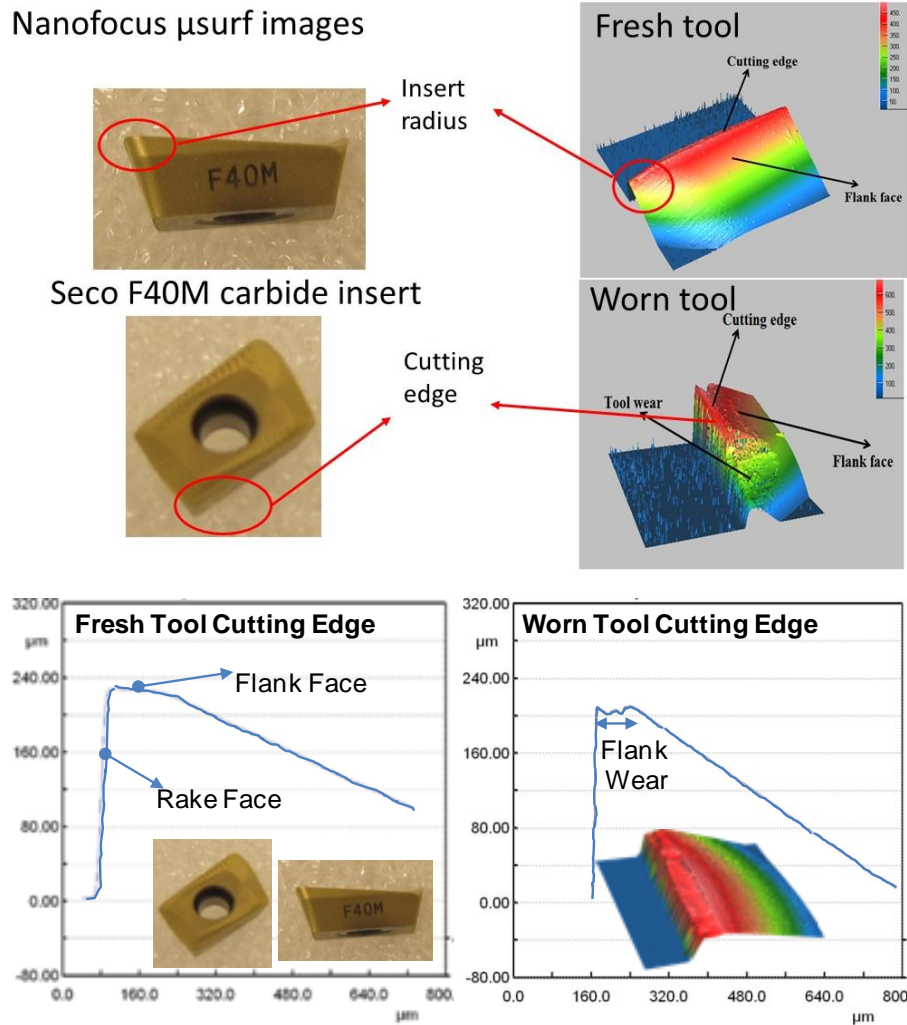
Figure 5-2: Cutting insert and Nano Focus image in turn-milling

Seco 32mm diameter end mill tool with three F40M inserts, which are proper for machining of difficult to cut materials, was used for Waspoloy, Inconel 718 and Ti6Al4V tool life experiments. Since the cutting tool has three inserts, the turn-milling wear results are normalized in order to compare with conventional turning data. The normalization procedure is performed by dividing the elapsed cutting time by three (number of teeth). Seco 50mm diameter face mill tool with four Seco Duratomic MP2500 inserts, which are proper for machining of steels, was used for AISI 1050 steel tool life experiments. In order to perform the same normalization procedure, the elapsed cutting time was divided by four. Detailed information about mentioned test and

measuring equipments are given in Section 2. Cutting test parameters were given onto corresponding test result graph in this section. V_c, f_z, a_e, and a_p represent cutting speed, feed per tooth, feed per workpiece revolution, and axial depth of cut respectively.

5.2. Experimental results and analysis

5.2.1. Machinability of Inconel 718

Figure 5-3 shows the tool wear results of Inconel 718 for both turn-milling and conventional turning operations. Metallurgical properties of Inconel 718 were given in Section 2 in detail.

Figure 5-3: Tool wear results for Inconel 718 in different cutting conditions

As it can be clearly seen from the graph that tool life is increased noticeably in turn-milling compared to conventional turning. Even dry cutting condition for turn-milling, which gives the worst tool life, has almost two times better tool life than conventional turning with fluid. As expected, coolant condition plays an essential role on tool wear in turn-milling. Turn-milling with flood provides almost four times higher tool life as compared to conventional turning with flood. MQL provides longer tool life results as compared to flood or dry cutting conditions [49]. In addition to its cooling effect, MQL enables lubrication effect which caused to decreased friction in cutting region.

5.2.2. Machinability of Waspaloy

Figure 5-4 illustrates the tool wear results of Waspaloy for both turn-milling and conventional turning operations. Detailed information about metallurgical properties of Waspaloy were given in Section 2 in detail.
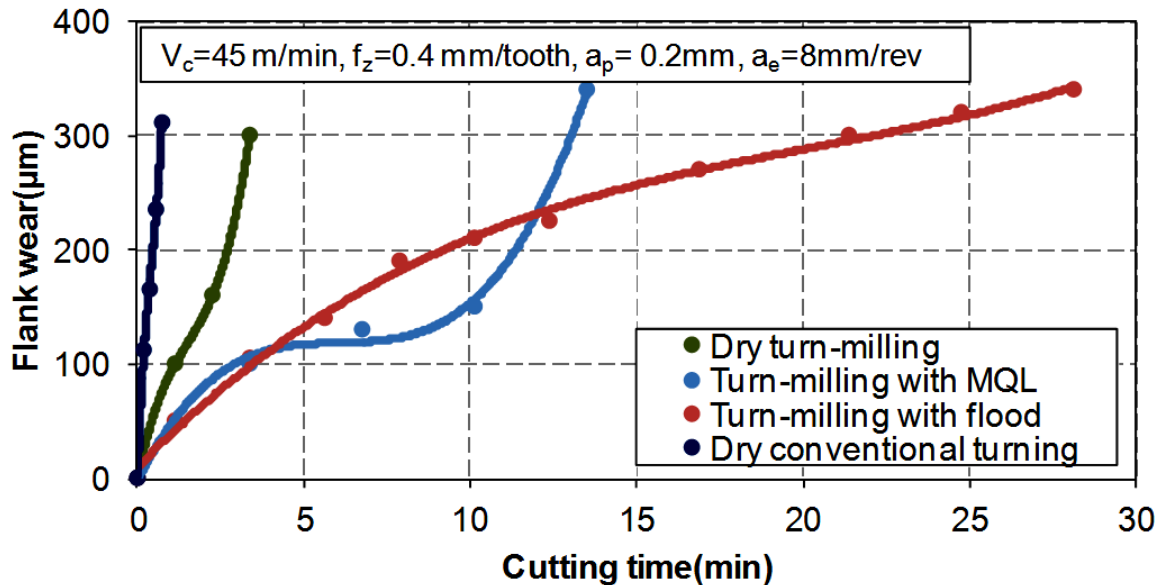
Figure 5-4: Tool wear results for Waspaloy in different cutting conditions

Machining of Waspaloy is highly difficult because of its exceptional mechanical properties. The principal characteristics of nickel-based super alloys such as Waspaloy and Inconel 718 are high phase stability of face-centered cubic nickel matrix and outstanding strength retention up to 70% of melting point [50]. The cutting inserts may break in dry cutting conditions instantly. It can be obviously seen from the graph that tool life is prolonged considerably, more than 25 times turn-milling with flood coolant. Moreover, even in dry turn-milling condition of Waspaloy, which gives the worst tool life result, provides five times better tool life conversely to conventional turning for the same cooling condition.

5.2.3. Machinability of Ti6Al4V

Figure 5-5 illustrates the tool wear results of Ti6Al4V for both turn-milling and conventional turning operations. Metallurgical properties of Ti6Al4V were given in Section 2.

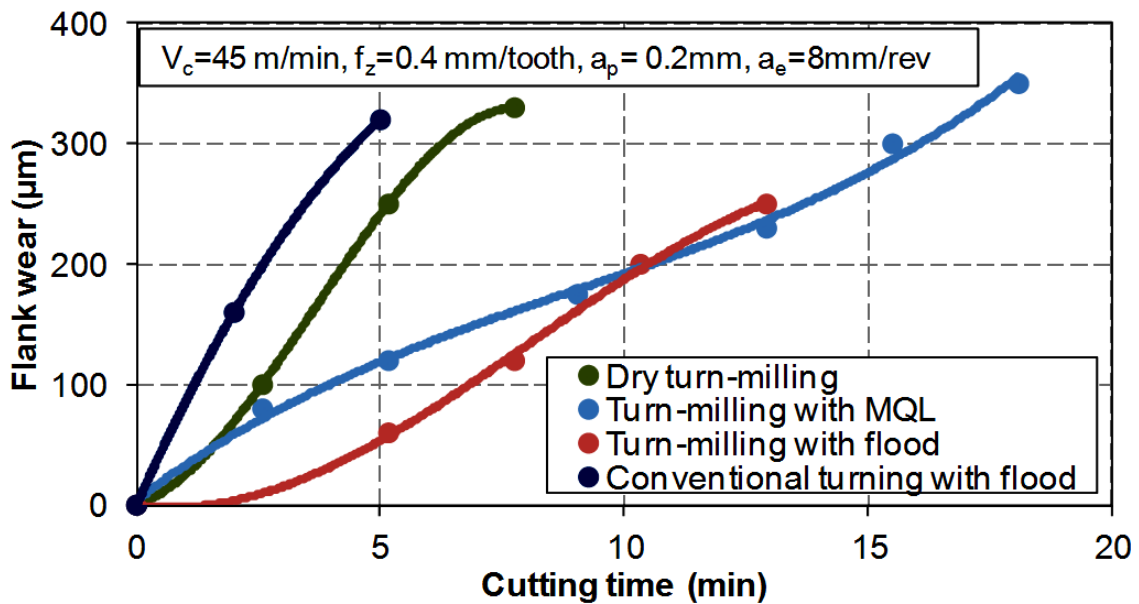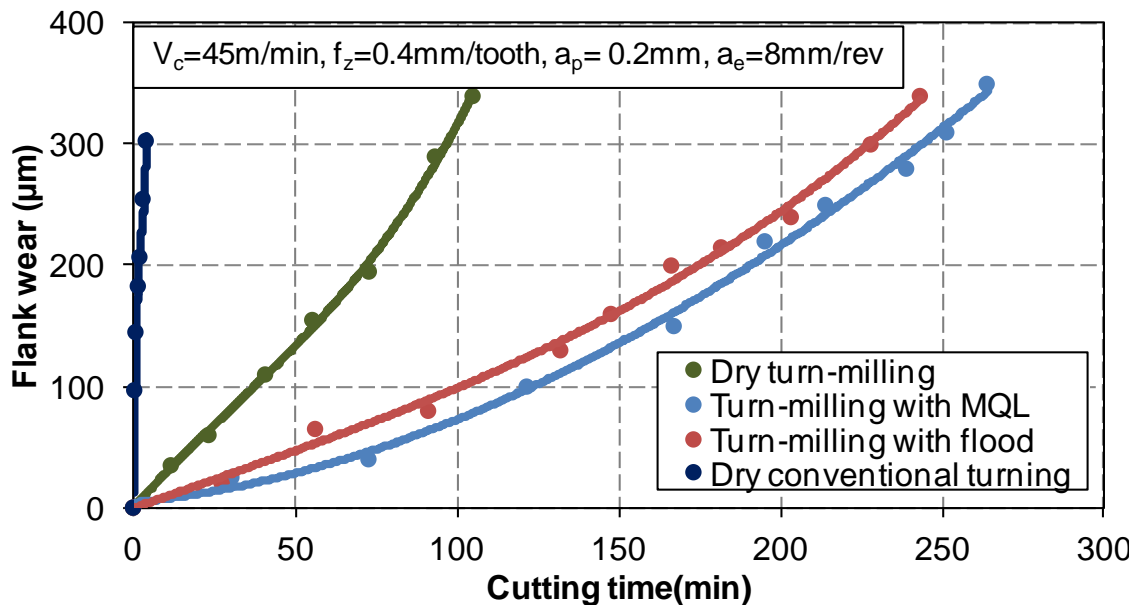Figure 5-5: Tool wear results for Ti6Al4V in different cutting conditions

It can be clearly seen from the graph that coolant plays a key role for machinability similar to the cases for other difficult to machine materials. Although dry turn-milling results in the worst tool life conversely to other cooling conditions, it still provides more than 25 times longer tool life in comparison to the conventional turning. When all of the workpiece materials tool life results for both cutting processes are taken into consideration, the most outstanding result was obtained from Ti6Al4V machining.

5.2.4. Eccentricity effect on tool life

As discussed earlier eccentricity has a non-negligible effect on turn-milling process parameters. Contact length between tool and workpiece directly depends on eccentricity parameter as shown in Figure 5-6.
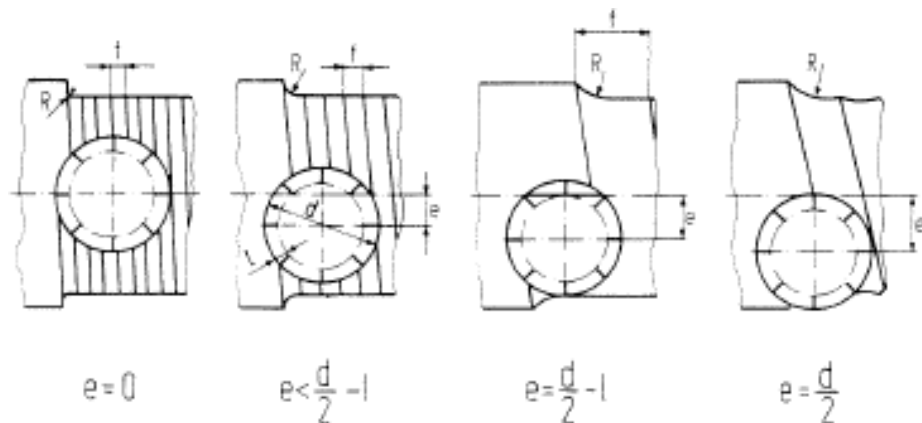
Figure 5-6: Positions of cutting tool and workpiece depends on eccentricity

Optimum eccentricity value, which gives the maximum projected length of tool onto workpiece, can be calculated as follows;

$$e_{opt} = R_t - L_n \qquad (5.1)$$

where R_t and L_n are the tool radius and minor cutting edge length of the tool insert, respectively. In order to observe the eccentricity effects on tool life, Seco 50mm diameter face mill tool with four teeth which has 4 mm minor cutting edge length was used.
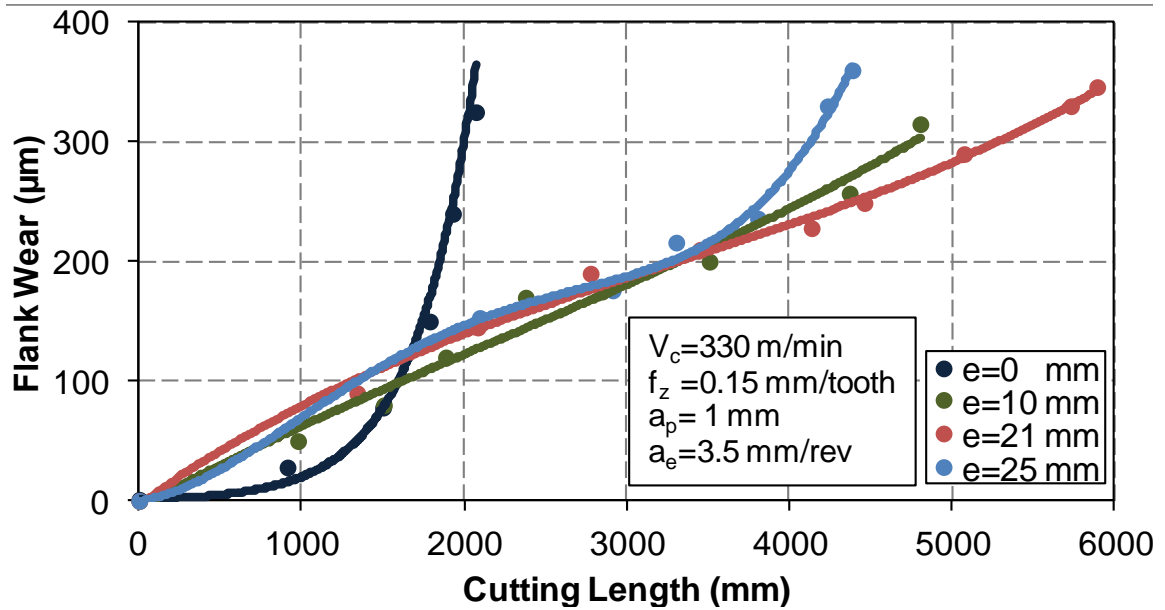
Figure 5-7: Eccentricity effect on tool life

The comparisons of the different eccentricity with tool flank wear can be seen in Figure 5-7. By using Eq. 5.1 the optimum eccentricity is selected as e_{opt}=21mm, by this means the engagement length of tool and workpiece becomes maximum, and the cutting pressure is well-distributed onto tool [24]. This is an important outcome as it shows that the maximum tool life is obtained for e=21mm case. Increasing eccentricity up to optimal value results in increasing tool life. When eccentricity equals to cutting tool radius, which is upper limit for eccentricity, the engagement length between cutting tool and workpiece reduces substantially. Since only the small portion of the cutting tool participated in cutting, excessive cutting pressure are exerted on side edge of the tool. Because of this statement, tool life for e=25mm case gives the worst result compared to other eccentric conditions. As a final observation, when the eccentricity is increased from zero to the optimum value, more than two times longer tool life can be obtained.

5.2.5. Inclination angle effect on tool life

Inclination angle, represented as *β* and illustrated in Figure 5-8, is one of the parameters which can be defined in turn-milling thanks to the multi-axis flexibility of the operation.
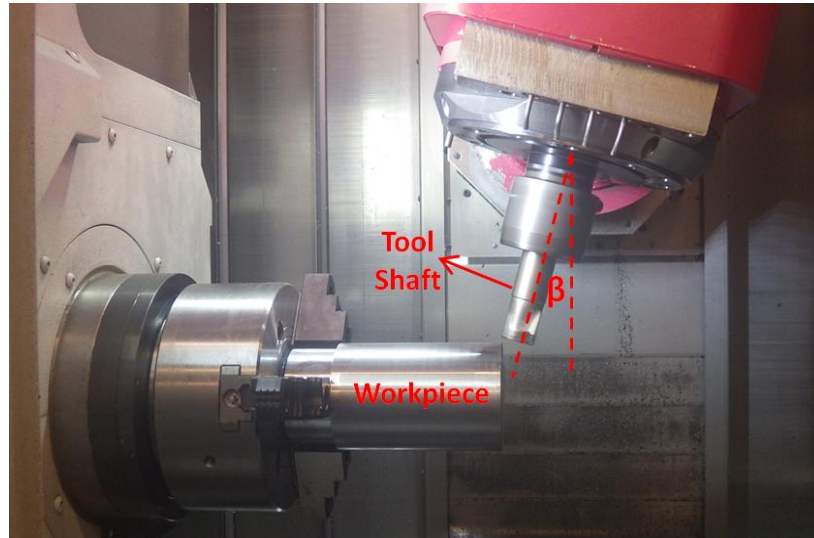
Figure 5-8: Representation of inclination angle (*β*) on Mori Seiki NTX2000 machine tool

In order to define this parameter, tool spindle must have *B* axis movement as shown in Figure 5-8. In analogy to the eccentricity parameter, inclination angle affects the contact length between tool and workpiece.
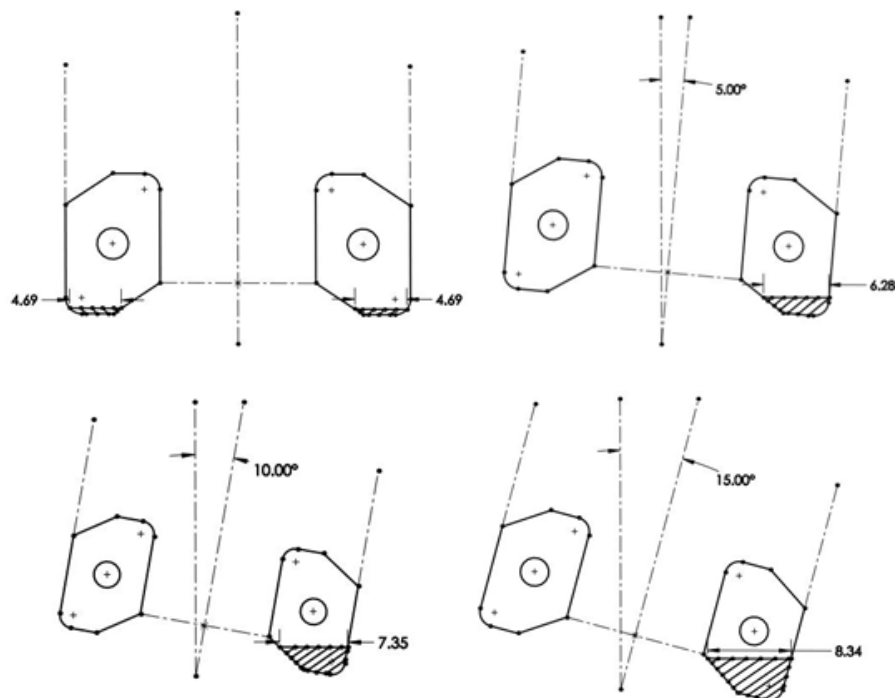
Figure 5-9: The relationship between inclination angle and contact length

Similar studies were done by other researchers for different machining operations like self propelled rotary turning. In one of these studies, it was stated that tool life increases by increasing inclination angle [49]. Thus, it can be clearly obtained that corresponding angle has an effect on tool life as shown in Figure 5-10.
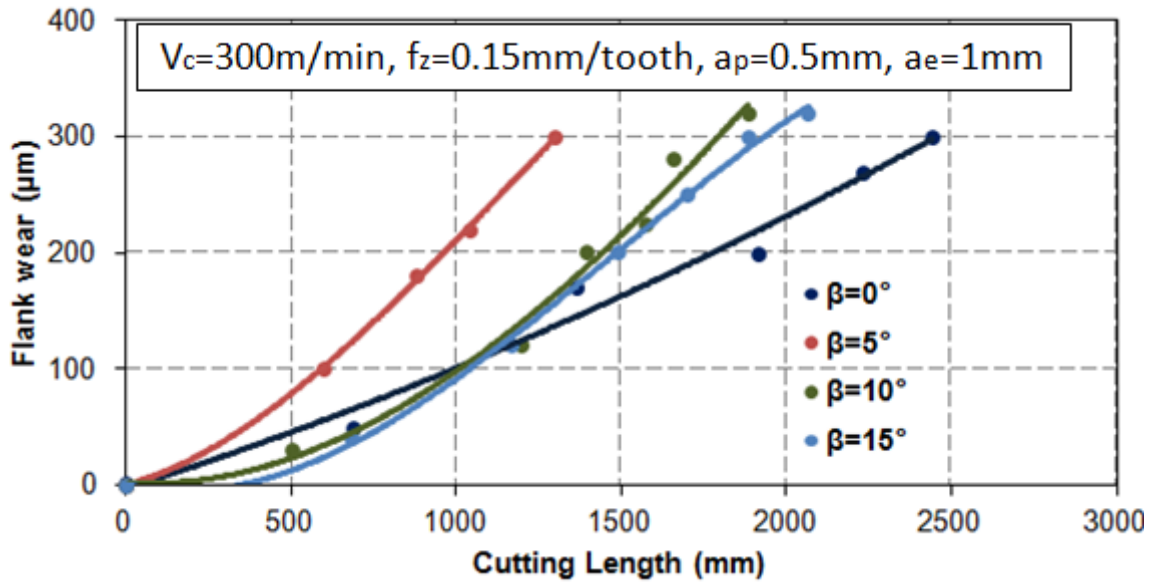
Figure 5-10: Inclination angle effect on tool life

Observing the results given in graph, it can be deduced that tool life increases by increasing inclination angle except $\beta = 0$ case. Although for the $\beta = 0$ case contact length seems minimum, total contact length is obtained as maximum because of the participation of other cutting insert as shown in Figure 5-9. As a result of the increasing contact length, cutting pressure is well-distributed and tool life is prolonged. Contrary to other studies for different machining operations, $\beta = 0$ case result in the longest tool life for turn-milling.

5.3. Summary

From the point of tool life, advantages of orthogonal turn-milling operations are presented in this section. For this purpose, tests were conducted in both orthogonal turn-milling and conventional turning with the same cutting conditions and compared with each other. In every scenario, it can be easily obtained that turn-milling has striking superiority to the conventional turning. As an example, 25 times longer tool life can be achieved by using orthogonal turn-milling in machining of Ti6Al4V. Besides the other advantages, this application obviously shows the economic return of the turn-milling applications.

CHAPTER 6

6. SUGGESTIONS FOR FUTURE RESEARCH

Most of required models for evaluation and selection of machining strategies in orthogonal turn-milling operations are proposed in this thesis. However, there are still points of improvement. In this section, presented recommendations may contribute to improve accuracy and ease of applicability of the models.

- Process geometry and mechanics of orthogonal turn-milling are presented in this thesis. These studies can be improved to more general turn-milling operations where the tool has more complexity (serrated, tapered, variable pitch, ball end mill etc.).

- The deviation between experimental and simulated results for cutting force including eccentricity comes from the edge force coefficient variations. Constant edge force coefficient was used in cutting force calculations, thus this parameter should be calibrated with respect to different eccentricities for more precise calculation.

- Presented surface roughness models can be extended by considering different cutting tool and insert geometries. In addition, cutting tool and workpiece vibrations can be added to the proposed form error models in order to obtain more accurate and realistic predictions.

- Tool life experiments with different cooling strategies such as cryogenic cooling, can be implemented on difficult-to-machine materials.

- Due to the axial and circumferential feed rates, cutting tool follows a helical path on workpiece in orthogonal turn-milling. Proposed models and predictions such as cutting forces, form errors, power/torque can be simulated throughout this tool path.

By simulating the desired tool path, process parameter's variations can be obtained throughout the corresponding tool path.

- The precision of machining processes are affected by the positioning accuracy of the cutting tool with respect to the workpiece and the relative structural deformations between them. Thus, static and dynamic deformations between the cutting tool and workpiece should be modeled.

- Thermal damages and residual stresses can influence component characteristics including fatigue life, corrosion resistance and part distortion. The functional behavior of machined components can be improved or impaired by residual stresses. That's why, residual stresses should be modeled.

- Tangential and co-axial turn-milling operations which are other types of turn-milling process can be modeled with the same procedure and methodology.

CHAPTER 7

7. CONCLUSIONS AND DISCUSSIONS

Turn-milling is one of the most flexible and reliable operations and it is preferred in industries which require high productivity and geometrical accuracy. Selecting process parameters properly is the key factor for increasing productivity and preventing poor surfaces, tool breakages and machine tool failures. Unpredicted high cutting forces and chatter type vibrations can lead to these unwanted situations. Process models are obtained possible process parameters by using geometrical and analytical models. Developed process models show that productivity of turn-milling can be improved by optimization of cutting parameters. In this thesis, the mechanics of orthogonal turn-milling including eccentricity is presented analytically and experimental investigation of the process is demonstrated for different materials and cutting conditions. From theoretical and experimental studies performed in this research the following conclusions can be drawn:

- Turn-milling is a relatively new machining operation and the definition of cutting parameters are different than the ones in traditional turning and milling. Moreover, due to the multi-axis flexibility of the process, there are variety of process parameters. Thus, a clear identification of the process geometry is required in order to conceive the operation. As an example, eccentricity, tilt angle, circumferential feed parameters are unfamiliar for conventional processes.
- Definition of engagement limits and uncut chip geometry are crucial from cutting force, chatter dynamics and cutting temperature points of view. That's why modeling of uncut chip geometry is proposed for orthogonal turn-milling. The contact area

between cutting tool and workpiece is identified and analytically calculated including eccentricity effect for instantaneous rotational angle of the cutting tool.

- Depends on the chip geometry definitions, cutting force model is evaluated for orthogonal turn-milling process by using semi-analytical force model which uses orthogonal to oblique transformation procedure of orthogonal turning data. Cutting experiments for verification of proposed force model were conducted on multi-tasking machine tool. It is obtained that experimental and analytical results are well agree with each other. Additionally, cutting forces increase with a_p and a_e and decrease with r_n and e.

- Due to the simultaneous tool and workpiece rotations, turn-milling generates non-cylindrical surfaces. Corresponding polygon shape cross section, which is one of the form errors of turn-milling, named as circularity. Although, circularity is an inevitable form error, it's degree strictly depends on the r_n ratio. If r_n ratio increases, the deviation from ideal circle decreases. By increasing n_t or decreasing n_w, r_n can be increased. Additionally, diminishing r_n also decrease the circumferential surface roughness.

- Feed per workpiece parameter is one of the main factors which directly affects productivity and surface quality at the same time. Increase in a_e can improve productivity which comes at the cost of increased cusp height. On the other hand, cusp height is an avoidable phenomenon by selecting a_e up to a critical value. By this means, productivity can be increased without observing any cusp on the machined surface. As a result, by using analytical models presented in this paper, MRR can be optimized based on the desired surface quality.

- There are two feed rates in turn-milling. The axial feed (a_e) defines the radial depth of cut whereas feed (f_z) in turn-milling corresponds to the feed rate in conventional milling. As a result, cutting tool follows a helical path which causes circumferential surface roughness. Circumferential surface roughness consists of cusp height and circularity form errors. Due to their effect on cusp height and circularity, a_e and r_n also have significant effect on the circumferential surface roughness. Up to a certain value of a_e the circumferential roughness is equal to the circularity error and increases by decreasing r_n. However, beyond that value, the circumferential surface roughness increases dramatically by a_e.

- Prolonged tool life is one of the crucial advantages of turn-milling operations. In some scenarios, by using turn-milling process 25 times longer too life (normalized for number of cutting edge and indexing) was obtained compared to the ones obtained from conventional turning process for the same cutting conditions. Intermitted characteristics of turn-milling helps to maintain low cutting temperatures and improve tool life. Moreover, it can be obviously understood from the cutting experiments that usage of coolant whether cutting fluid and MQL increase tool life drastically. Eccentricity, which is one of the main focuses of this thesis, is an important parameter in terms of tool life. Experimental studies point out that optimum eccentricity provides the best results for tool life. Additionally, increasing tilt angle also contributes to the tool life positively.

7.1. Original contributions of the thesis

For orthogonal turn-milling, as the first time in the literature;

- Cutting forces are calculated by semi-analytical force model which uses orthogonal to oblique transformation. This study is published at International Journal of Machine Tools and Manufacture [16]. Eccentricity effect on cutting force is modeled analytically. This work is accepted for presentation at 16th International Conference on Machine Design and Production [17] , which is one of the most important conferences in machining research.
- Analytical models for cusp height and circumferential surface roughness including eccentricity effect are developed. The developed models are used for process simulation and MRR optimization. The proposed scheme is accepted for presentation at 6th CIRP Conference on High Performance Cutting [24], which is another important conference in machining research.
- In machining of difficult-to-cut materials, tool life results obtained from conventional turning and multi-tasking machining operations for different cutting conditions are compared to each other. These results are accepted for presentation at 4th Machining Innovation Conference [27], which is another important conference in machining research. This study is extended by investigating eccentricity effect on tool life and published at The International Journal of Advanced Manufacturing Technology [35].

REFERENCES

[1]   Moriwaki, T. 2008, Multi-functional machine tool. CIRP Annals-Manufacturing Technology, 57:736–749.

[2]   Jovane F., Koren Y., Boren C. R. 2003, Present and Future of Flexible Automation: Towards New Paradigm. Annals of the CIRP, 52/2:543-560.

[3]   Koren Y., Heisel U., Jovane F., Moreiwaki T., Pritschow G., Ulsoy G., VanBrussel H. 1999, Reconfigurable Manufacturing Systems. Annals of the CIRP, 48/2:527-540.

[4]   Landers R. G., Min H. B., Koren Y. 2001, Reconfigurable Machine Tools. Annals of the CIRP, 50/1:269-274.

[5]   Dmgmori, NTX 2000 Series, www.dmgmori-usa.com/ntx-series/ntx2000s. Accessed October 2014.

[6]   Mazak, Multi-tasking machines, www.mazakusa.com/machines/process/multi-tasking. Accessed October 2014.

[7]   Aspinwall D. K., Dewes J. M., Burrows J. M., Paul M. A. 2001, Hybrid High Speed Machining (HSM): System Design and Experimental Results for Grinding/HSM and EDM/HSM. Annals of the CIRP, 50/1:145-148.

[8]   Nakagawa T., Suzuki K., Uematsu T., Kimura M. 1988, Development of a New Turning Center for Grinding Ceramic Materials. Annals of the CIRP, 37/1:319-322.

[9]   Sandvik Coromat, Turn-milling application, www.sandvik.coromant.com. Accessed May 2014.

[10]   Estman L., Merdol D., Brask K.G., Kalhori V., Altintas Y. 2013, Development of Machining Strategies for Aerospace Components, Using Virtual Machining Tools. New Production Technologies in Aerospace Industry, Springer International Publishing pp. 63-68.

[11]   Espirit 2011, Simplified 5-Axis Machining, www.dptechnology.com. Accessed December 2014.

[12]   Choudhury S. K., Bajpai J. B. 2005, Investigation in orthogonal turn-milling towards better surface finish. Journal of Materials Processing Technology, 170/3:487-493.

[13]   Filho C., Martins J. 2012, Prediction of cutting forces in mill turning through process simulation using a five-axis machining center. The International Journal of Advanced Manufacturing Technology, 58/1-4:71-80.

[14] Merchant E. 1945, Mechanics of the Metal Cutting Process I. Orthogonal Cutting and a Type 2 Chip. Journal of Applied Physics, 16/5:267-275.

[15] Schulz G., Spur G. 1990, High speed turn-milling—a new precision manufacturing technology for the machining of rotationally symmetrical workpieces. Annals of the CIRP, 39/1:107–109.

[16] Karaguzel U., Uysal E., Budak E., Bakkal M. 2014, Analytical modeling of turn-milling process geometry, kinematics and mechanics. International Journal of Machine Tools and Manufacture, DOI:10.1016/j.ijmachtools.2014.11.014.

[17] Karaguzel U., Uysal E., Budak E., Bakkal M. 2014, Modeling of Turn-Milling Processes for Increased Productivity. The 16th International Conference on Machine Design and Production.

[18] Qui W., Liu Q., Yuan S. 2015, Modeling of cutting forces in orthogonal turn-milling with round insert cutters. The International Journal of Advanced Manufacturing Technology, 64/1-4:475-486.

[19] Choudhury S. K., Mangrulkar K. S. 2000, Investigation of orthogonal turn-milling for the machining of rotationally symmetrical work pieces. Journal of Materials Processing Technology, 99:120–128.

[20] Zhu L., Haonan L., Wansan W. 2013, Research on rotary surface topography by orthogonal turn-milling. The International Journal of Advanced Manufacturing Technology, 69/9-12:2279-2292.

[21] Vedat S., Ozay C. 2007, Analysis of the surface roughness of tangential turn-milling for machining with end milling cutter. Journal of Materials Processing Technology, 186/1:279-283.

[22] Kopac J., Pogacnik M. 1997, Theory and practice of achieving quality surface in turn milling. International Journal of Machine Tools and Manufacture, 37/5:709-715.

[23] Yuan S. M., Zheng W. W. 2012, The surface roughness modeling on turn-milling process and analysis of influencing factors. Applied Mechanics and Materials, 117:1614-1620.

[24] Uysal E., Karaguzel U., Budak E., Bakkal M. 2014, Investigating eccentricity effects in turn-milling operations. 6th CIRP International Conference on High Performance Cutting, HPC 2014, Procedia CIRP, 44:176-181.

[25] Neagu C., Gheorghe M., Dumitrescu A. 2005, Fundamentals on face milling processing of straight shafts. Journal of Materials Processing Technology, 166/3:337-344.

[26] Stephenson D. A., Ali A. 1992, Tool temperatures in interrupted metal cutting. Journal of Engineering for Industry by ASME, 114:127-136.

[27] Karaguzel U., Olgun U., Uysal E., Budak E., Bakkal M. 2014, High performance turning of high temperature alloys on multi-tasking machine tools. New Production Technologies in Aerospace Industry. Springer International Publishing pp. 1-9.

[28] Huang C., Cai Y. L. 2013, Turn-milling parameters optimization based on cutter wear. Advanced Materials Research, 602:1998-2001.

[29] Ezugwu E. O., Wang Z. M. 1995, Titanium alloys and their machinability-a review. Journal of Materials Processing Technology, 68:262-274.

[30] Kappmeyer G., Hubig C., Hardy M., Witty M., Busch M. 2012, Modern machining of advanced aerospace alloys - enabler for quality and performance. Procedia CIRP, 1:28-43.

[31] Ezugwu E. O. 2005, Key improvements in the machining of difficult-to-cut aerospace superalloys. International Journal of Machine Tools and Manufacture, 45: 1353–1367.

[32] Machado A. R., Wallbank J. 1997, The effect of extremely low lubricant volumes in machining. Wear, 210/1:76-82.

[33] Wang Z. Y., Rajurkar K. P. 2000, Cryogenic machining of hard-to-cut materials. Wear, 239/2:168-175.

[34] Ezugwu E. O., Bonney J. 2004, Effect of high-pressure coolant supply when machining nickel-base, Inconel 718, alloy with coated carbide tools. Journal of Materials Processing Technology, 153:1045-1050.

[35] Karaguzel U., Olgun U., Uysal E., Budak E., Bakkal M. 2014, Increasing tool life in machining of difficult-to-cut materials using nonconventional turning processes. The International Journal of Advanced Manufacturing Technology, Springer London pp.1-12.

[36] Pogacnik M., Kopac J. 2000, Dynamic stabilization of the turn-milling process by parameter optimization. Proceedings of the Institution of Mechanical Engineers, Part B: Journal of Engineering Manufacture, 214/2:127-135.

[37] Klocke F., Klink A., Veselovac D., Aspinwall D. K., Soo S. L., Schmidt M., Schilp J., Levy G., Kruth J. P. 2014, Turbomachinery component manufacture by application of electrochemical, electro-physical and photonic processes. Annals of CIRP, 63:703-726.

[38] Rolls Royce, Trent 800 Series, www.rolls-royce.com/civil/products/800Series. Accessed December 2014.

[39] Sreejith P.S. 2008, Machining of 6061 aluminum alloy with MQL, dry and flooded lubricant conditions. Materials Letters, 62/2:276-278.

[40] Wang W. P. 1988, Solid Modeling for Optimizing Metal Removal of Three-dimensional NC End Milling. Journal of Manufacturing Systems, 7/1:57-65.

[41] Budak E., Altintas Y., Armarego E. J. A. 1996, Prediction of Milling Force Coefficients from Orthogonal Cutting Data. Journal of Manufacturing Science and Engineering, 118:216-224.

[42] Altintas Y. 2012, Manufacturing automation: metal cutting mechanics, machine tool vibrations, and CNC design. Second Edition, Cambridge University Press, New York.

[43] Zorev N.N. 1966, Metal Cutting Mechanics. Pergamon Press.

[44] Masuko M. 1956, Fundamental Researches on the Metal Cutting – Force Acting on a Cutting Edge and Its Experimental Discussion. Transactions Japanese Society of Mechanical Engineers, 22:371-377.

[45] Albrecht P. 1960, The Ploughing Process in Metal Cutting. Trans ASME Journal of Engineering for Industry, pp. 348-358.

[46] Budak E. 1994, Mechanics and Dynamics of Milling Thin Walled Structures, PHD Thesis, The University of British Columbia, Vancouver, Canada.

[47] Astakhov V. P. 2006, Effects of the cutting feed, depth of cut, and workpiece (bore) diameter on the tool wear rate. The International Journal of Advanced Manufacturing Technology, 34/7-8:631-640.

[48] Olgun U., Budak E. 2013, Machining of Difficult-to-Cut-Alloys Using Rotary Turning Tools. Procedia CIRP, 8:81-86.

[49] Faverjon P., Rech J., Leroy R. 2013, Influence of minimum quantity lubrication on friction coefficient and work-material adhesion during machining of cast aluminum with various cutting tool substrates made of polycrystalline diamond, high speed steel, and carbides. Journal of Tribology, 135/4:041602.

[50] Davis J. R. 2000, ASM Speciality Handbook: Nickel, Cobalt, and Their Alloys, The Materials Information Society.